Neuron, Vol. 19, 403–419, August, 1997, Copyright ©1997 by Cell Press

Release-Activated Ca^{2+} Transport in Neurons of Frog Sympathetic Ganglia

Zoltán Cseresnyés, Alexander I. Bustamante, Michael G. Klein, and Martin F. Schneider
Department of Biochemistry and Molecular Biology
University of Maryland School of Medicine
Baltimore, Maryland 21201

Summary

Frog sympathetic ganglion neurons exhibit a novel Ca^{2+} uptake mechanism, release-activated calcium transport or RACT, which is manifest in both cytosolic and store [Ca^{2+}] signals as greatly accelerated Ca^{2+} uptake after Ca^{2+} release from internal stores. RACT is activated by Ca^{2+} release but not by Ca^{2+} entry and serves to selectively refill Ca^{2+} stores after release. RACT lowers cytosolic [Ca^{2+}] with a rate constant about 1.6 times that of the SERCA pump with empty ER. RACT is thapsigargin-insensitive, was eliminated by ryanodine, but was not affected by blocking mitochondrial or plasma membrane Ca^{2+} transport. A Ca^{2+} flux model with RACT in the ER membrane reproduced the cytosolic and store [Ca^{2+}] responses to all stimuli.

Introduction

Cytosolic [Ca^{2+}] serves as a signal for modulating a wide range of cellular activities, both across the spectrum of diverse cell types and within a particular cell. The mechanisms by which Ca^{2+} can regulate a variety of different functions within an individual cell are thus of considerable general interest. Some examples of specificity of neuronal Ca^{2+} signaling appear to involve spatial localization of the effective [Ca^{2+}] signal to the neighborhood of specific sites mediating individual functions (Ginty, 1997). Thus, locally elevated [Ca^{2+}] in the neighborhood of a particular type of Ca^{2+} channel might specifically modulate the activity of an enzyme localized in the vicinity of that channel (Deisseroth et al., 1996).

Here, we show that a novel Ca^{2+} transport mechanism, termed release-activated calcium transport or RACT, which markedly accelerates the rate of removal of cytosolic Ca^{2+} after Ca^{2+} release is selectively activated by Ca^{2+} release from the endoplasmic reticulum (ER) in frog sympathetic ganglion neurons. Release activation of transport is apparently a highly localized phenomenon, since it is produced by ER Ca^{2+} release but not by a plasma membrane Ca^{2+} influx giving rise to a similar elevation of global cytosolic [Ca^{2+}]. We propose that the release-activated Ca^{2+} transport mechanism is located in the ER membrane, and that it may serve the important functions of rapidly terminating the [Ca^{2+}] transient after strong activation of Ca^{2+} release and of maintaining intracellular Ca^{2+} stores by selectively reloading them after release, thereby preventing depletion of intracellular Ca^{2+}. Maintenance of intracellular stores may be especially important during oscillatory signaling in neurons (Friel and Tsien, 1992a; Kuba et al., 1992; Nohmi et al., 1992b; Friel, 1995) and possibly in other cell types as well (Barry and Cheek, 1994).

Preliminary results of our findings were published in abstract form (Cseresnyés et al., 1996, 1997, Biophys. J., abstracts).

Results

Ca^{2+} Release Activates Ca^{2+} Transport

Depolarization of an isolated frog sympathetic ganglion neuron by exposure to 50 mM K^+ Ringer's solution produced a rapid rise of [Ca^{2+}] to a plateau that continued for the duration of the high K^+ exposure (Figure 1A, peak 1), presumably due to activation of voltage-dependent plasma membrane Ca^{2+} channels and the resulting large Ca^{2+} influx across the plasma membrane (Lipscombe et al., 1988; Friel and Tsien, 1992b, 1994). The decay of [Ca^{2+}] after return to 2 mM K^+ was biphasic, exhibiting an initial rapid phase of decay followed by a slower final phase. A subsequent brief exposure of the same neuron to 10 mM caffeine, which releases Ca^{2+} from internal stores via ryanodine receptor (RyR) Ca^{2+} release channels (Endo et al., 1970; Lipscombe et al., 1988; Bezprozvanny et al., 1991; Friel and Tsien, 1992a, 1992b; Marrion and Adams, 1992; Nohmi et al., 1992b; Ogawa, 1994), resulted in a brief [Ca^{2+}] transient (Figure 1A, peak 2) having about the same peak amplitude as the high K^+ response. However, in contrast to the biphasic decay of [Ca^{2+}] after high K^+, the decay of [Ca^{2+}] after caffeine exhibited a monophasic fast decay. The rate constant for the decay of [Ca^{2+}] after caffeine was about 15× greater than the rate constant for the final decay of [Ca^{2+}] after high K^+, even though the peak elevations were similar in the two responses. Continued influx of Ca^{2+} after removing the high K^+ solution was not involved in producing the slow final decay of [Ca^{2+}] after high K^+, since the slow phase remained in Ca^{2+}-free Ringer's solution (peak 3). The time courses of the high K^+ or caffeine [Ca^{2+}] transients observed here resemble those reported previously for similar types of activation (Friel and Tsien 1992a, 1992b, 1994; Nohmi et al., 1992a; Verkhratsky and Shmigol, 1996). In the present experiments, the mean rate constant of the final decay of [Ca^{2+}] was $0.033 \pm 0.009\ s^{-1}$ ($n = 14$) after high K^+, and $0.25 \pm 0.03\ s^{-1}$ ($n = 17$) after caffeine.

When a neuron was briefly exposed to caffeine immediately following an exposure to 50 mM K^+ (Figure 1B, peak 2), the resulting Ca^{2+} release by caffeine caused a second peak of [Ca^{2+}] superimposed on the slow phase of decay of [Ca^{2+}] after the high K^+ response. The subsequent decay of [Ca^{2+}] after caffeine was fast, similar to that after caffeine alone (cf. Figure 1A, peak 2), and much faster than after high K^+ alone in the same (Figure 1B, peaks 1 and 3) or in other neurons (e.g., Figure 1A, peaks 1 and 3). Thus, the slow transport of Ca^{2+} out of the cytosol after Ca^{2+} entry was greatly accelerated after Ca^{2+} release by caffeine. The potentiated Ca^{2+} transport activated by Ca^{2+} release rapidly lowered not only the Ca^{2+} released by caffeine but also

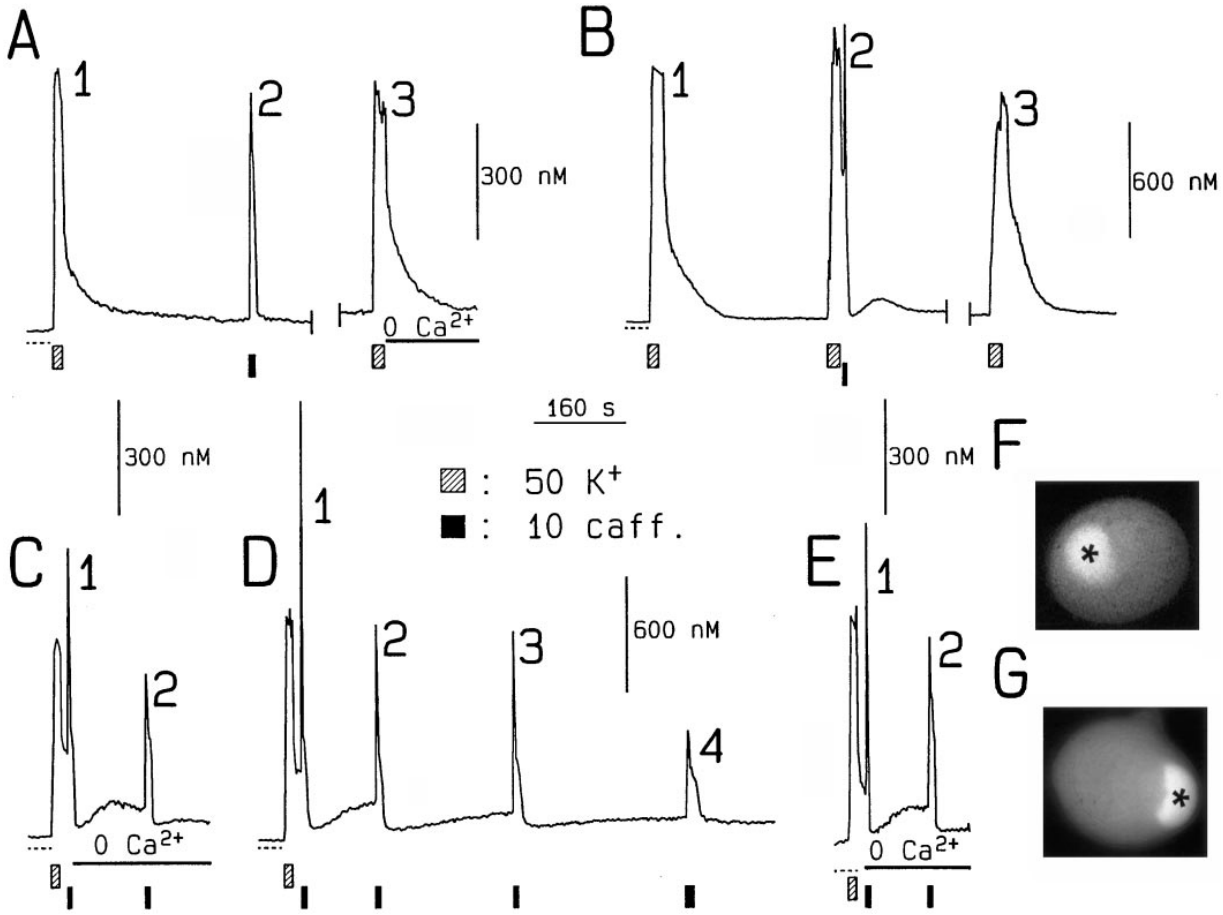

Figure 1. Slow and Fast Decay of $[Ca^{2+}]$ after Depolarization-Induced Influx and Caffeine-Evoked Release of Ca^{2+}

(A) High K^+ solution (striped bar; peak 1) and 10 mM caffeine in Ringer's solution (solid bar; peak 2) were applied to a neuron (the length of each bar corresponds to the duration of exposure to the indicated solution). The high K^+ application was repeated (peak 3) after a 30 min wash (indicated by a break in the record), and the decay phase was monitored in the absence of extracellular Ca^{2+} (solid line beneath the record). The dashed line below the start of the record denotes zero $[Ca^{2+}]$ in this and all other panels and figures.

(B) A brief high K^+ exposure (peak 1) was applied alone or was followed after a short (4 s) wash in normal Ringer's solution by 10 mM caffeine (peak 2), leading to the appearance of a second peak, a fast decay of $[Ca^{2+}]$, and then a delayed rise of $[Ca^{2+}]$. After washing the cell with normal Ringer's solution for 7 min (break), the high K^+ response was evoked again without caffeine (peak 3).

(C) Following a high K^+ pulse and a 14 s wash with normal Ringer's solution, 10 mM caffeine was applied (peak 1). The extracellular solution was then changed to Ca^{2+}-free Ringer's (indicated by the solid line beneath the curve) for the duration of the delayed rise of $[Ca^{2+}]$. Caffeine exposure was then repeated (peak 2).

(D) A high K^+ exposure was followed by a 16 s wash and a caffeine exposure (peak 1). During the secondary rise of $[Ca^{2+}]$, 10 mM caffeine was applied (peak 2). During the small delayed rise following peak 2, 10 mM caffeine was applied again (peak 3). The control caffeine response (peak 4) was considerably smaller in amplitude.

(E) Experimental test of the release-activated fast uptake in a neuron microinjected with fura-2 pentapotassium salt. High K^+ exposure was followed by a 14 s wash with normal Ringer's and exposure to 10 mM caffeine before $[Ca^{2+}]$ reached the resting level (peak 1). The extracellular solution was then switched to a Ca^{2+}-free Ringer's (denoted by the solid line below the record). The caffeine exposure was repeated (peak 2) on top of the delayed rise of $[Ca^{2+}]$. The time calibration applies to (A) through (E).

(F) Fluorescence image of a neuron loaded by exposure to 2 μM fura-2 AM for 20 min at room temperature. The image was detected at 510 nm for excitation at 358 nm, the Ca^{2+} independent wavelength of fura-2. The dye distribution is restricted to the cytosol and the nuclear region of the cell. The nucleus (asterisk) is brighter presumably because of a higher effective concentration of the dye in the nucleus, due to dye exclusion from the ER and other nonnuclear organelles.

(G) Another neuron was microinjected with a pipette containing 1 mM fura-2 free acid, and the image was taken at 510 nm for excitation at 358 nm. The nucleus (asterisk) is again brighter than the cytosol, similar to (F). The nonnuclear area of the cell shows homogeneous fluorescence, indicating uniform dye distribution and thus uniform nonorganellar cytoplasmic space in the cell. The width of each image in Figures 1 and 2 is 47 μm. Panels (A) through (G) are from different neurons.

the cytosolic Ca^{2+} remaining from the preceding Ca^{2+} influx during high K^+ depolarization (Figure 1B). Further observations (below) indicate that the accelerated transport of Ca^{2+} out of the cytosol after Ca^{2+} release is due to potentiated uptake into the endoplasmic reticulum.

Delayed Release of Accumulated Ca^{2+} after Release-Activated Transport

The rapid decay of $[Ca^{2+}]$ when caffeine was applied during the decay of $[Ca^{2+}]$ after high K^+ was often followed by a delayed, slow rise and fall of $[Ca^{2+}]$ (Figure

1B, following peak 2). The delayed rise of $[Ca^{2+}]$ was also observed in the absence of extracellular Ca^{2+} (Figure 1C, following peak 1) and thus could not be due to Ca^{2+} influx from the extracellular solution, but must instead have been caused by a delayed release of Ca^{2+} ions previously accumulated in internal stores during the activated Ca^{2+} transport after Ca^{2+} release. The delayed rise of $[Ca^{2+}]$ after Ca^{2+} release was terminated by a caffeine-induced Ca^{2+} release (Figures 1C and 1D, peak 2), and a subsequent second delayed rise of $[Ca^{2+}]$ was also terminated by Ca^{2+} release (Figure 1D, peak 3). If the delayed rise of $[Ca^{2+}]$ is due to release of accumulated Ca^{2+} as the release activation of Ca^{2+} transport declines with time after release, reactivation of fast Ca^{2+} transport by a second Ca^{2+} release would be expected to terminate the delayed rise of $[Ca^{2+}]$ as observed. Since the time course of the slow phase of decline of $[Ca^{2+}]$ after exposure to high K^+ (above) and that of the decline of the delayed rise in $[Ca^{2+}]$ are similar, the same mechanism may be involved in generating both slow phenomena. The effect of caffeine on the delayed rise of $[Ca^{2+}]$ after activation of potentiated transport also suggests that the activated transport system moves Ca^{2+} back into the caffeine-sensitive Ca^{2+} pool.

Release-Activated Ca^{2+} Transport Monitored Using Microinjected Fura-2

In order to confirm the cytosolic and nuclear origin of the dye and thus of the $[Ca^{2+}]$ signals after fura-2 acetyoxymethyl ester (AM) loading, $[Ca^{2+}]$ transients were also monitored in some neurons using microinjected membrane-impermeant fura-2 salt (see Experimental Procedures). Both the 50 mM K^+ response and the peak, rapid decline, and secondary rise of $[Ca^{2+}]$ in response to caffeine after high K^+ (Figure 1E, peak 1) in fura-2 injected cells resemble those of the fura-2 AM loaded cells (cf. Figure 1C). The secondary rise of $[Ca^{2+}]$ was obvious in all five neurons studied after microinjection with fura-2, even in the absence of extracellular Ca^{2+} (Figure 1E), and was sensitive to caffeine (Figure 1E, peak 2) as in the fura-2 AM loaded cells (above). Thus, possible fluorescence signals arising from fura-2 trapped in intracellular compartments (Kao, 1994) after loading with fura-2 AM apparently did not significantly influence the observed time course of $[Ca^{2+}]$ after high K^+ and/or caffeine. At the end of each of the five experiments with microinjected fura-2, the cells were depolarized in the presence of 10 mM $MnCl_2$, which enters neurons via plasma membrane Ca^{2+} channels. Depolarization in Mn^{2+} rapidly quenched 95%–96% of the fura-2 fluorescence at 358 nm, indicating that at least 95%–96% of fura-2 was in the cytoplasm and thus not compartmentalized.

Intracellular Distribution of Ca^{2+} Indicators

The intracellular distribution of fura-2 fluorescence for excitation at the isosbestic wavelength after fura-2 AM loading of neurons was brighter in the nucleus than in the cytosol (Figure 1F), consistent with dye exclusion from organelles outside the nucleus and a predominantly cytosolic and nuclear origin of the fura-2 fluorescence. The distribution of fura-2 fluorescence in injected neurons (Figure 1G) was also predominantly cytosolic and nuclear, as should be the case after injection of the membrane-impermeant salt, and was very similar to that of fura-2 AM-loaded neurons (Figure 1F), confirming the predominantly cytosolic and nuclear location of fura-2 after AM loading. In order to directly examine the rate of Ca^{2+} transport into internal stores in sympathetic neurons, we loaded some neurons by exposure to fluo-3FF AM (TEFLABS, Austin, TX; Patent# 5,516,911, May 14, 1996), using conditions (Golovina and Blaustein, 1997) that promote indicator sequestration into internal organelles. Fluo-3FF has a relatively low Ca^{2+} affinity (K_D = 42 μM), which is appropriate for monitoring $[Ca^{2+}]$ within neuronal stores. Like fluo-3 (Terasaki and Sardet, 1991; Z. C., A. I. B., M. G. K., and M. F. S., unpublished data), fluo-3FF is sequestered into internal organelles. The typical fluorescence image of a sympathetic neuron loaded with fluo-3FF under these conditions (Figure 2Aa) exhibits a bright store-like pattern (Hofer and Machen, 1993; Short et al., 1993) with a dark nuclear region, indicative of low cytosolic and nuclear fluorescence and high store fluorescence. The fluorescence distribution in Figure 2Aa was just opposite of that in Figure 1F, consistent with a complimentary distribution of indicator fluorescence for the different loading procedures and indicators. Comparison of the bright field (Figure 2Ab) and fluorescence images of the same neuron indicates that the high $[Ca^{2+}]$ store signal occupied most but not all of the nonnuclear regions of the neuron.

Monitoring Store $[Ca^{2+}]$ Confirms Release-Activated Ca^{2+} Transport

The whole-cell fluorescence of neurons loaded with fluo-3FF under conditions that promote indicator sequestration in internal stores was monitored during stimuli that promote uptake or release of store Ca^{2+}. The fluo-3FF fluorescence of such neurons gradually increased during exposure to high K^+ and then slowly declined after wash out of high K^+ (Figure 2B), consistent with gradual Ca^{2+} loading into the stores as a result of elevated cytosolic $[Ca^{2+}]$ (Figures 1A and 1B, peaks 1 and 3) during exposure to high K^+ and slow loss of the extra accumulated store Ca^{2+} as cytosolic $[Ca^{2+}]$ returned to resting levels after removal of high K^+. Thus, Ca^{2+} influx across the plasma membrane during exposure to high K^+ caused increases in both cytosolic (Figure 1) and store (Figure 2B) $[Ca^{2+}]$. Brief exposure of a fluo-3FF loaded neuron to caffeine caused a rapid decrease in fluorescence (Figure 2C, peak 1), consistent with rapid loss of Ca^{2+} from the ER due to strong activation of Ca^{2+} release channels by caffeine. Ca^{2+} release from the ER thus caused opposite changes in cytosolic (Figure 1A, peak 2) and store (Figure 2C) $[Ca^{2+}]$ signals, consistent with Ca^{2+} movement from store to cytosol and with the cytosolic and store location of fura-2 (Figure 1) and fluo-3FF (Figure 2). The caffeine-induced change in fluo-3FF fluorescence was not an artifact of caffeine–dye interaction, since exposure of fluo-3FF loaded neurons to caffeine caused no change in fluorescence after block of calcium release by ryanodine (not shown). Fluo-3FF accumulated in mitochondria made little contribution to the total fluo-3FF fluorescence signal, since in cells

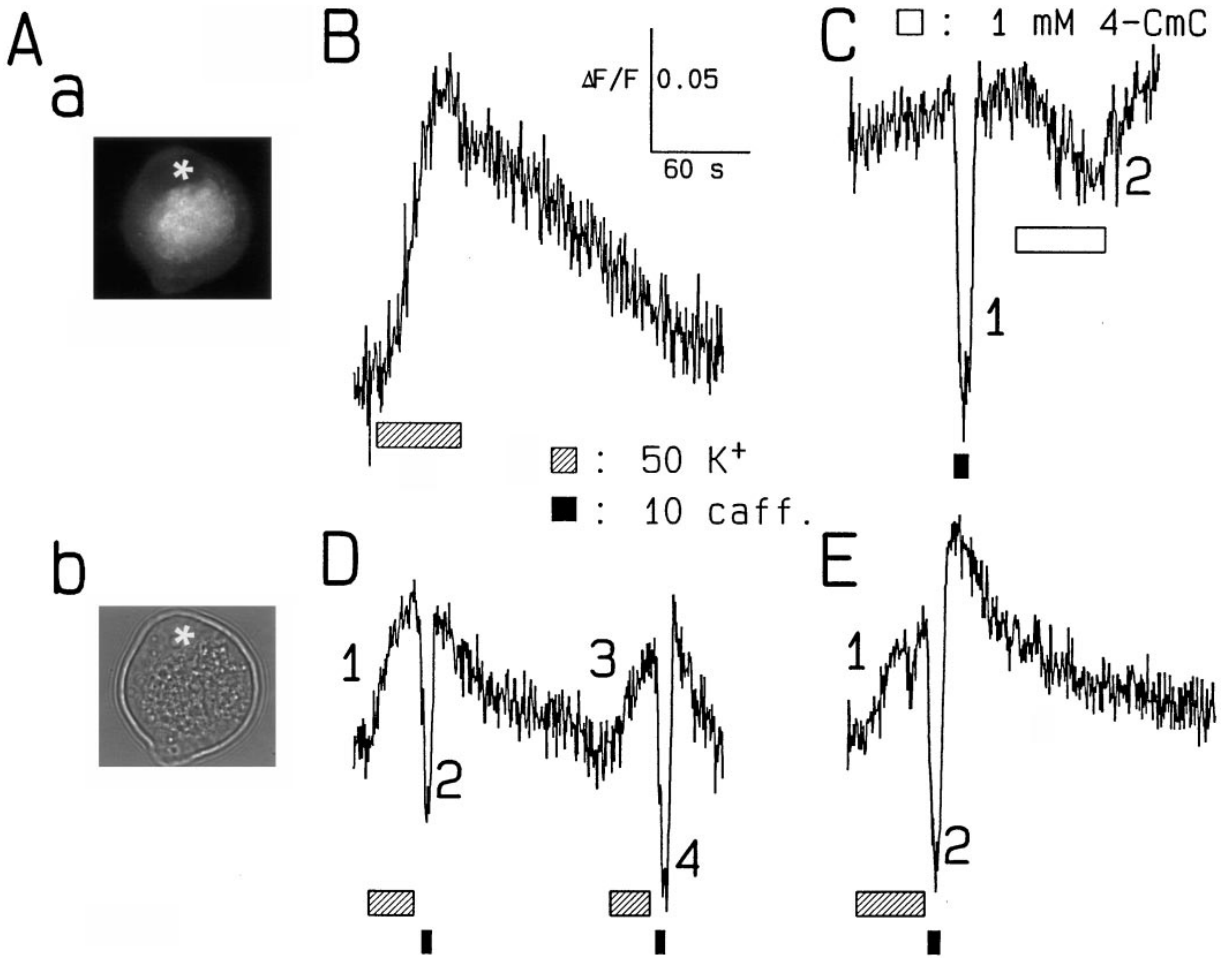

Figure 2. Fluo-3FF Monitoring of [Ca^{2+}] in Intracellular Stores

(Aa) Fluorescence image detected at 535 nm (excitation at 490 nm) of a neuron loaded by exposure to 4 μM fluo-3FF AM at 35°C for 90 min. The nucleus (asterisk) is dark. The bright area outside the nucleus indicates the store region of the neuron due to the preferential loading of the dye into the intracellular compartments and the higher [Ca^{2+}] characterizing the calcium stores inside these compartments.

(Ab) Bright field image of neuron in Aa.

(B) Whole-cell fluorescence at 490 nm excitation from another neuron loaded with fluo-3FF, under the same conditions as in (A). Application of high K^+ caused a gradual rise of store fluorescence. When K^+ was decreased to 2 mM, the store signal slowly declined and reached the level before the high K^+ pulse.

(C) A different neuron, loaded as in (A), was exposed to 10 mM caffeine (peak 1) and showed a sharp decrease in store fluorescence that lasted as long as the caffeine was present and was followed by a quick recovery when caffeine was washed out. Exposure of this cell to 1 mM 4-chloro-*m*-cresol (4-CmC; bar underneath the record) resulted in a slower response of store fluorescence (peak 2).

(D) High K^+ exposure caused a slow increase of fluo-3FF store signal of another neuron (peak 1). 10 mM caffeine was then applied (peak 2) after a 5 s wash with 2 mM [K^+] Ringer's. The whole sequence of high K^+ and caffeine exposures was repeated on the same cell to test reproducibility (peaks 3 and 4).

(E) Another neuron showed an overshoot of the fluorescence signal after caffeine (peak 2) was washed out following a high K^+ application (peak 1).

pretreated with mitochondrial-blockers FCCP (1 μM) and oligomycin (10 μM), the same time course of fluorescence was detected as in Figures 2D and 2E (not shown).

The increase in fluo-3FF fluorescence when a neuron was washed with caffeine-free solution after a brief exposure to caffeine (Figure 2C, peak 1) was much faster than the increase in fluorescence during exposure to high K^+ (Figure 2B), consistent with a marked potentiation of Ca^{2+} uptake after Ca^{2+} release. When a neuron was exposed to high K^+ and then briefly exposed to caffeine (Figure 2D, peaks 1 and 2), the rate of increase in fluo-3FF fluorescence after caffeine was much faster than during high K^+, directly confirming that calcium transport into internal stores was activated after release. The sequence of slow Ca^{2+} accumulation during exposure to high K^+, rapid Ca^{2+} release during caffeine, and rapid reuptake of Ca^{2+} after caffeine was reproducible (Figure 2D, peaks 3 and 4). Exposure to caffeine after high K^+ caused store fluorescence to exceed that prior to caffeine in some neurons (Figure 2E, following peak 2), consistent with accumulation of excess Ca^{2+} from the cytosol after activation of release-activated transport. The fluo-3FF store signals obtained during and after Ca^{2+} release by caffeine (Figure 2) are similar in

speed but opposite in direction to the fura-2 cytosolic $[Ca^{2+}]$ signals during and after Ca^{2+} release (Figure 1), and thus directly confirm our interpretation that the rapid fall in cytosolic $[Ca^{2+}]$ following Ca^{2+} release (Figure 1) is due to rapid accumulation of Ca^{2+} into intracellular stores (Figure 2).

Rapid Transport after Caffeine Is Not Activated by Changes in cAMP

In addition to potentiating calcium-induced calcium release by direct interaction with the RyR Ca^{2+} release channels, caffeine and related methylxanthines might also modulate cAMP-dependent neuronal functions due to inhibition of phosphodiesterase (Butcher and Sutherland, 1962). We therefore examined the effects of altering cellular levels of cAMP on the cytosolic $[Ca^{2+}]$ signals. Direct application of the membrane permeant cAMP analog dibutyryl cAMP (d-cAMP) immediately after high K^+ did not cause Ca^{2+} release and did not increase the rate of Ca^{2+} transport during the decay of $[Ca^{2+}]$ after high K^+ (Figure 3A, peak 3). The continued presence of d-cAMP did not appreciably modify the rapid decay of $[Ca^{2+}]$ in the caffeine response after high K^+ (peak 4). Application of 100 μM of the phosphodiesterase inhibitor 3-isobutyl-1-methylxanthine (IBMX), which does not activate the RyR calcium release channel (Zidichousky et al., 1989; Nohmi et al., 1992b), was also without effect on the decay of $[Ca^{2+}]$ after high K^+ or on the rapid decay of $[Ca^{2+}]$ after caffeine with or without high K^+ (data not shown). Thus, the effects of caffeine in increasing the rate of Ca^{2+} transport do not seem to be mediated via modification of cytosolic cAMP levels, as noted previously regarding the effects of caffeine on bullfrog sympathetic ganglion neurons (Friel and Tsien, 1992b).

Other xanthines that release Ca^{2+} from the ryanodine-sensitive Ca^{2+} pools of the ER (Müller and Daly, 1993) also activated calcium transport. 1,7-Dimethylxanthine

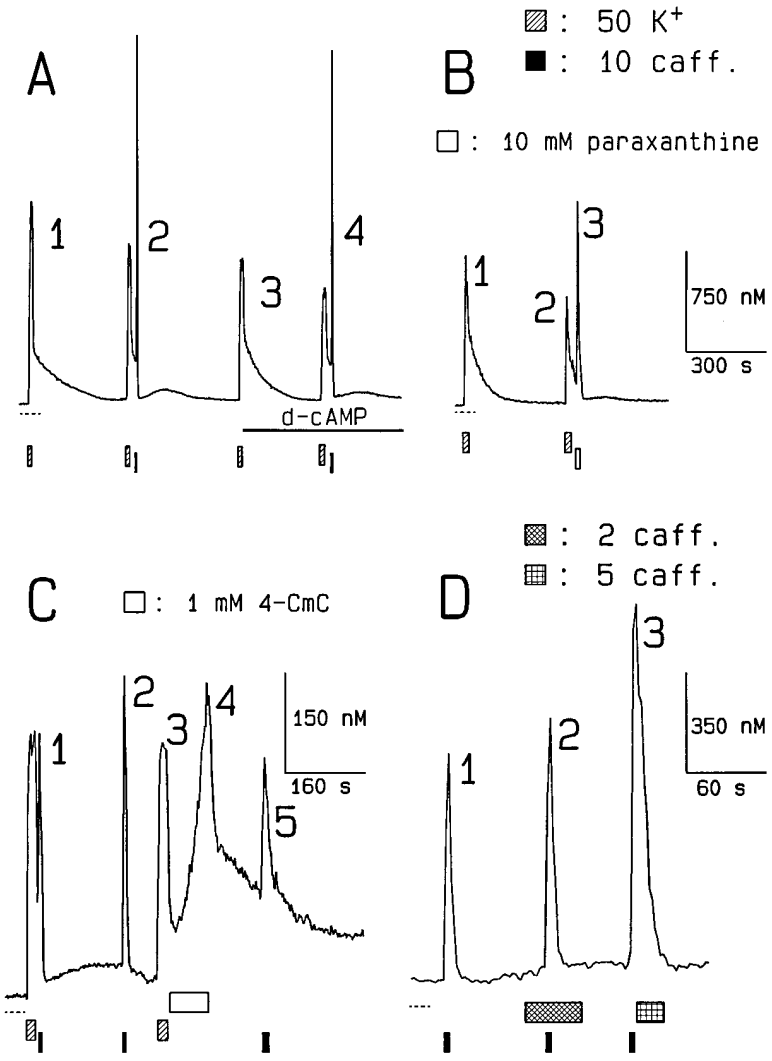

Figure 3. Caffeine and Other Methylxanthines Activate the Fast Ca^{2+} Uptake via Releasing Ca^{2+} from the ER, Not by Increasing the cAMP Concentration

(A) The first high K^+ response (peak 1) was repeated and was followed by a short caffeine exposure (peak 2) after a 20 s wash with Ringer's solution. When the secondary rise and fall of $[Ca^{2+}]$ following this caffeine response was over, high K^+ solution was applied again and was then washed with Ringer's solution containing 1 mM dibutyryl-cyclic AMP (d-cAMP; bar beneath the record). Peak 4, which contains a high K^+ and a caffeine exposure with a 20 s wash in between, was detected in the continuous presence of 1 mM d-cAMP.

(B) Two high K^+ exposures were applied, the first one as a control (peak 1), while the second one (peak 2) was followed by the application of 10 mM 1,7-dimethylxanthine (paraxanthine; peak 3) after a 16 s wash. A small delayed rise of $[Ca^{2+}]$ is also present on the record, following peak 3.

(C) The effect of another ER Ca^{2+} releasing agent, 4-CmC, on the time course of $[Ca^{2+}]$ in another neuron. After a high K^+ followed by caffeine (peak 1) and caffeine alone (peak 2), 1 mM 4-CmC was applied (peak 4) after a high K^+ response (peak 3). Caffeine response was tested again 100 s after the removal of 4-CmC (peak 5).

(D) The effect of increased ER Ca^{2+} leak on the time course of $[Ca^{2+}]$ response induced by 10 mM caffeine. After a control 10 mM caffeine response (peak 1), the cell was exposed to 2 mM caffeine that did not induce an appreciable change of $[Ca^{2+}]$ (bar under the record). Ten millimolar caffeine was then applied (peak 2), and the washout was done with Ringer's containing 2 mM caffeine (bar). The next 10 mM caffeine application (peak 3) was followed by a wash with 5 mM caffeine in Ringer's solution (bar under record). The decay rate constants of $[Ca^{2+}]$ after peaks 1, 2, and 3 were 0.39 s^{-1}, 0.33 s^{-1} and 0.17 s^{-1}, respectively, showing a significant slowing down of net Ca^{2+} uptake in the presence of partially activated RyR release channels.

(paraxanthine, 10 mM) caused a Ca^{2+} transient (Figure 3B, peak 3) that decayed rapidly and was followed by a small delayed rise of $[Ca^{2+}]$ (Figure 3B, after peak 3). The $[Ca^{2+}]$ peaks produced by 10 mM paraxanthine were larger in amplitude than those induced by 10 mM caffeine (not shown) as found for sarcoplasmic reticulum calcium release channel activation by these xanthines (Rousseau et al., 1988). Application of 1,3-dimethylxanthine (theophylline, 10 mM) and of 10 mM caffeine gave similar results (data not shown), consistent with the similar effects of theophyline and caffeine on sarcoplasmic reticulum Ca^{2+} channels incorporated into planar bilayers (Rousseau et al., 1988) and on PC12 cells (Müller and Daly, 1993).

The effects of several nonxanthine compounds known to activate RyR Ca^{2+} release channels in other systems (Palade, 1987; Zorzato et al., 1993; Herrmann-Frank et al., 1996) were also examined. The rise of $[Ca^{2+}]$ during application of 4-chloro-*m*-cresol (4-CmC; 1 mM) after high K^+ (Figure 3C, peak 4) was much slower than that produced by caffeine alone or by caffeine after high K^+ (peaks 2 or 1), indicating lower activation of release by 4-CmC than by caffeine. The decay of $[Ca^{2+}]$ after 4-CmC was also slower than after the preceding caffeine responses. Store fluorescence recordings with fluo-3FF demonstrated a much slower fall and rise of store $[Ca^{2+}]$ during and after 4-CmC application than those observed for caffeine application in the same neuron (Figure 2C, peaks 2 and 1, respectively), confirming that the slower cytosolic $[Ca^{2+}]$ changes with 4-CmC correspond to slower release and reuptake of Ca^{2+} from the stores. Other nonxanthine release activators (thymol, 1 mM; quercetin, 0.1 mM) gave even slower activation of Ca^{2+} release during application and slow decline of the resulting elevated $[Ca^{2+}]$ after removal (not shown), indicating even slower development and wash out of the drug effects.

Maintained Activation of ER Ca^{2+} Channels Prevents Rapid Ca^{2+} Accumulation

At 100 s after wash out of 4-CmC, the decay of $[Ca^{2+}]$ after caffeine was also slow (Figure 3C, peak 5), indicating the possibility of maintained release channel activation from the preceding application of 4-CmC shunting the potentiated Ca^{2+} transport activated during Ca^{2+} release by caffeine after 4-CmC. The decay of $[Ca^{2+}]$ after 10 mM caffeine was slower when the caffeine was washed off with 2 or 5 mM caffeine (Figure 3D, peaks 2 and 3) than when washed off with caffeine-free solution (peak 1), indicating that maintained activation of release can indeed slow the uptake of $[Ca^{2+}]$ after release activation.

A long exposure to 10 mM caffeine resulted in a $[Ca^{2+}]$ transient characterized by a significantly slower decay of $[Ca^{2+}]$ during caffeine exposure than after a short exposure (not shown; Friel and Tsien, 1992b). Since the continued presence of caffeine keeps the RyR Ca^{2+} channels activated for the whole period of the caffeine exposure, the potentiated transport mechanism is probably shunted to a significant extent. Thus, even if the rate constant for Ca^{2+} uptake into the caffeine-sensitive Ca^{2+} pool is high due to the parallel action of sarco/endoplasmic reticulum calcium ATPase (SERCA) pumps and the activated transport system, in the continued presence of activation of Ca^{2+} release the open RyR Ca^{2+} channels do not allow the ER to accumulate any net excess Ca^{2+}, as demonstrated by the slower decay of $[Ca^{2+}]$ during a long caffeine exposure. These results thus provide additional support for the ER membrane location of the release-activated calcium transport system.

Plasma Membrane and Mitochondrial Ca^{2+} Transport Are not Activated by Ca^{2+} Release

Both the delayed rise of $[Ca^{2+}]$ in response to caffeine after high K^+ and the store $[Ca^{2+}]$ signals after release suggest that Ca^{2+} was rapidly transported into internal stores after Ca^{2+} release (above). In order to confirm this conclusion, we examined the effects of inhibitors of plasma membrane Ca^{2+} transport systems. Application of 1 mM La^{3+} Ringer's solution to a neuron significantly slowed the decay of $[Ca^{2+}]$ after high K^+ (Figure 4A, peak 2), consistent with inhibition of the plasma membrane Ca^{2+} pump (PMCA) by La^{3+} and with a significant contribution of PMCA to the slow decay of $[Ca^{2+}]$ after high K^+ (Herrington et al., 1996). In contrast, 1 mM La^{3+} had no slowing effect on the rapid decay of $[Ca^{2+}]$ following Ca^{2+} release by caffeine after high K^+ (peak 3), indicating that PMCA did not contribute significantly to the activated Ca^{2+} transport after calcium release. Exposure of another neuron to Na^+-free, Ca^{2+}-free Ringer's solution caused a slight slowing of the decay of $[Ca^{2+}]$ after high K^+ (Fig 4B, peak 2), indicating that the Na^+/Ca^{2+} exchanger also contributed to the decay of $[Ca^{2+}]$ after high K^+. However, the Na^+-free, Ca^{2+}-free Ringer's had no effect on the rapid decay of $[Ca^{2+}]$ after high K^+ and caffeine (Figure 4B, peaks 3 and 4), showing that the plasma membrane Na^+/Ca^{2+} exchanger did not contribute significantly to the activated Ca^{2+} transport after Ca^{2+} release.

Mitochondria have been shown to accumulate and subsequently release significant quantities of Ca^{2+} in bullfrog sympathetic neurons, especially during and after relatively large and prolonged elevations of $[Ca^{2+}]$ (Friel and Tsien, 1994), and in other cell types as well (Gunter and Pfeiffer, 1990; Rizzuto et al., 1993, 1994; Huang and Chueh, 1996; Hehl et al., 1996; Herrington et al., 1996). In order to further define the possible internal membrane location of the activated Ca^{2+} transport after Ca^{2+} release, we therefore examined the effects of agents that dissipate the mitochondrial membrane potential (FCCP; CCCP; Friel and Tsien, 1994; Budd and Nicholls, 1996; Huang and Chueh, 1996; Herrington et al., 1996) and thus reduce mitochondrial Ca^{2+} accumulation and release, and of agents which inhibit the mitochondrial ATP synthase (oligomycin; Budd and Nicholls, 1996; Huang and Chueh, 1996). Application of 5 μM FCCP to a neuron during the slow decay of $[Ca^{2+}]$ after high K^+ caused a slight rise in $[Ca^{2+}]$ (Figure 4C, after peak 3), indicating mitochondrial inhibition. A subsequent application of caffeine caused a large calcium release and rapid decay of $[Ca^{2+}]$ (peak 4), as observed before mitochondrial inhibition (peak 2). The larger amplitude of peak 4 compared to peak 2 is consistent with

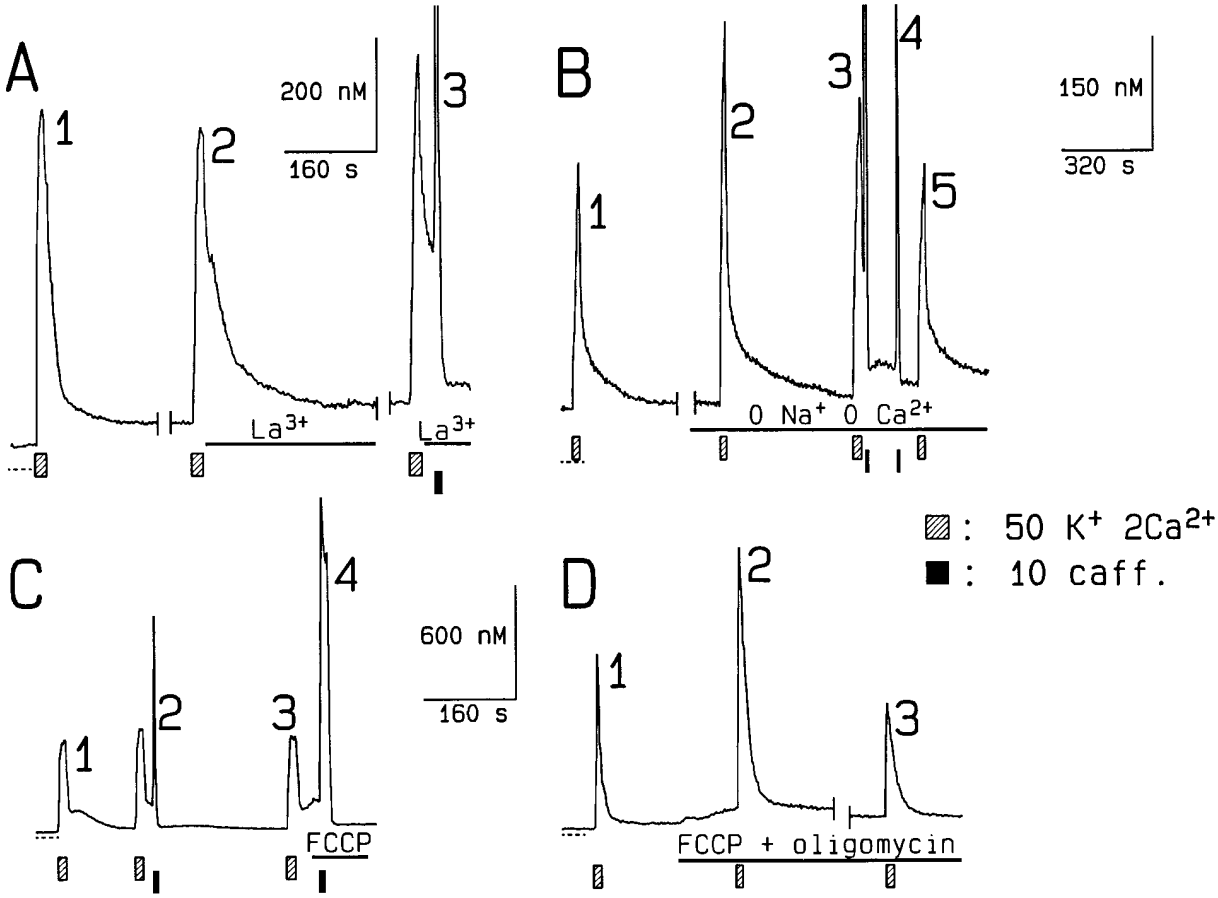

Figure 4. The Mechanism Responsible for the Fast Ca^{2+} Uptake Is Not Related to Either Plasma Membrane Ca^{2+} Transport or to Mitochondria

(A) The first high K^+ exposure (peak 1) was followed by a wash with normal Ringer's, while after the second high K^+ response (peak 2), the extracellular solution was a Ringer's containing the PMCA-blocker La^{3+} in form of 1 mM $LaCl_3$ (bar beneath the record). Since La^{3+} blocks the surface membrane Ca^{2+} channels as well, the La^{3+} exposure was followed by a wash with Ringer's solutions containing 5 mM sodium orthophosphate (Le Guennec et al., 1996) to override the La^{3+} effect (the break in the record corresponds to 4 min). The third K^+ response was also evoked in the presence of NaH_2PO_4 and was followed by a 20 s wash and then a caffeine exposure (peak 3), both with 1 mM La^{3+} in the Ringer's solutions.

(B) After the control high K^+ response (peak 1), the extracellular solution was switched to an Na^+- and Ca^{2+}-free Ringer's (bar beneath the record) to eliminate most of the surface membrane Na^+/Ca^{2+} exchanger activity. The break in the record corresponds to 5 min. The time constant of the slow component of the high K^+ response in the absence of Na^+ (peak 2; 2 mM Ca^{2+} was added back for the duration of the high K^+ exposure) was 120 s, twice as much as that of the control (peak 1, 60 s). Caffeine was applied shortly after a high K^+ exposure, followed by a 10 s wash in Na^+-free solution (peak 3). The caffeine exposure was repeated on top of the delayed rise and fall of $[Ca^{2+}]$ (peak 4) and was followed by a high K^+ exposure again (peak 5).

(C) The control high K^+ response (peak 1) had a rather well expressed plateau component, which was abolished when caffeine was applied following a 15 s wash after the repeated application of high K^+ (peak 2). When another high K^+ exposure (peak 3) was followed by application of mitochondrial uptake-blocker FCCP (5 μM, bar beneath the record), $[Ca^{2+}]$ showed an additional increase superimposed onto the plateau of the high K^+ response, a result of the block of mitochondrial Ca^{2+} uptake. Caffeine, still in the presence of FCCP, was applied again when the FCCP-induced increase of $[Ca^{2+}]$ reached a plateau (peak 4). The decay of $[Ca^{2+}]$ following the caffeine-induced release of Ca^{2+} had a fast time course.

(D) Mitochondrial uptake was blocked by 5 μM FCCP coapplied with 10 μM oligomycin to avoid the reverse activity of mitochondrial ATP synthase. The time constants of $[Ca^{2+}]$ decay after the high K^+ response in the absence of mitochondrial uptake (peaks 2 and 3) were similar to those of the control (peak 1): 17.1 s, 20.7 s, and 20.8 s for peaks 1, 2 and 3, respectively.

mitochondrial inhibition after FCCP and a mitochondrial contribution to cytosolic Ca^{2+} buffering before inhibition (Friel and Tsien, 1994).

In 23 neurons, the rate constant of decay of $[Ca^{2+}]$ after caffeine was measured under control conditions as well as after application of 1 or 5 μM FCCP or 4 or 10 μM CCCP. The average of rate constant ratios for these neurons was 0.89 ± 0.06, and the difference between the mean rate constants of control and FCCP/CCCP experiments was not significant. The maintained fast decay of $[Ca^{2+}]$ after calcium release under mitochondrial inhibition indicates that mitochondria were not involved in the potentiated transport after calcium release. Consequently, the mitochondrial contribution to Ca^{2+} removal was not taken into account in our further calculations of the Ca^{2+} transport rate constants of the SERCA pump and of the potentiated transport.

Continuous application of FCCP alone caused the

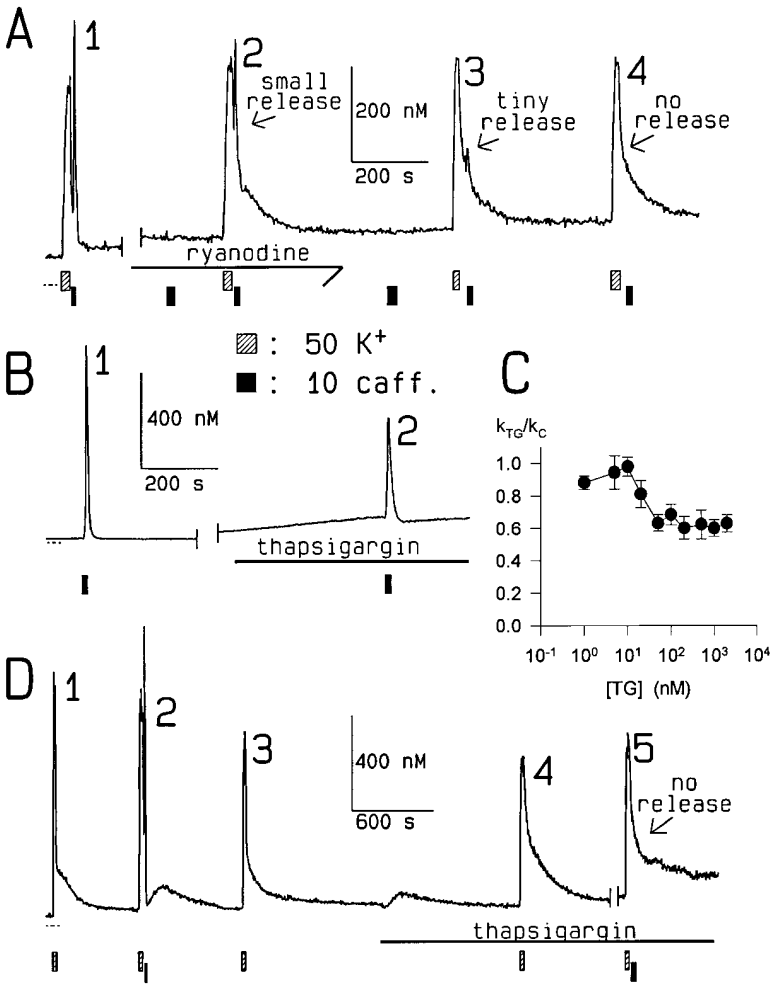

Figure 5. The Dependence of $[Ca^{2+}]$ Uptake Rate on Ryanodine and Thapsigargin during RACT

(A) Peak 1 consists of a high K^+ exposure followed by a 4 s wash and caffeine application. The gap in the record corresponds to 4 min. Ryanodine (20 μM) was applied extracellularly (indicated by the arrow beneath the record), starting 3 min before the end of the gap and continuing throughout the experiment. Caffeine was applied during the gap to activate RyRs (not shown), and the caffeine applied afterward did not release Ca^{2+} (bar before peak 2), indicating that the ryanodine effect was complete. Peak 2 starts with a high K^+ exposure, then a 4 s wash and a 10 mM caffeine pulse follow. Caffeine did not release Ca^{2+} when applied at the resting $[Ca^{2+}]$ level (bar between peaks 2 and 3). Ten minutes later, the high K^+ response was tested again (peak 3), when the high K^+ exposure was followed by a wash, then a caffeine pulse. Another test followed after 6 min (peak 4).

(B) Caffeine (10 mM) in normal Ringer's solution was applied (peak 1), then the cell was washed for 10 min (break in record). TG (200 nM) was applied, and caffeine was then added to the perfusing solution (peak 2) when the slow rise of $[Ca^{2+}]$, because of the TG exposure, was detected.

(C) Dose-response curve of TG-block of SERCA pumps. TG was applied from the extracellular side of 3–6 different cells at each TG concentration. The experiment to determine the TG effect on the decay rate of $[Ca^{2+}]$ after caffeine response was the same as for panel (B) of this figure.

(D) Peak 1 is the result of a high K^+ exposure, while peak 2 has a high K^+ pulse followed by an 8 s wash and caffeine application. Peak 3 is a high K^+ control. TG (200 nM; indicated by the solid line beneath the record) was applied and induced a transient rise of $[Ca^{2+}]$ (hump between peaks 3 and 4). After 15 min following the TG-induced rise of $[Ca^{2+}]$, a high K^+ pulse (peak 4) was applied. The next high K^+ response (peak 5) was followed by a caffeine application with a 14 s wash in between.

neurons to deteriorate relatively rapidly with time, presumably due to depletion of ATP supplies. Part of the rapid degradation of ATP after FCCP in intact neurons may be due to ATP hydrolysis by the mitochondrial ATP synthase working in reverse mode after dissipation of the mitochondrial membrane potential (Budd and Nicholls, 1996). Application of 5 μM FCCP together with 10 μM oligomycin to block mitochondrial ATP hydrolysis caused a slow rise in $[Ca^{2+}]$, indicating mitochondrial inhibition and calcium release (Figure 4D, before peak 2). The rate of decay of $[Ca^{2+}]$ after high K^+ was similar to the rate before mitochondrial inhibition, both 2 min (peak 2) and 6 min (peak 3) after mitochondrial inhibition. Thus, mitochondria do not appear to make a significant contribution to the slow decay of $[Ca^{2+}]$ after high K^+ under the conditions of brief K^+ exposures used in these studies. The limited role of mitochondrial Ca^{2+} transport under the conditions of our experiments was confirmed by the observation of similar store $[Ca^{2+}]$ signals during and after Ca^{2+} influx or during and after Ca^{2+} release by caffeine in the presence or absence of 1 μM FCCP plus 10 μM oligomycin (not shown).

Results similar to those in Figure 4 were observed in 4 out of 5 neurons exposed to 1 mM La^{3+}, 6 out of 8 neurons exposed to Na^+-free, Ca^{2+}-free Ringers solution, and 22 out of 31 neurons exposed to 1–5 μM FCCP or 4–10 μM CCCP. Thus, neither transport across the plasma membrane nor mitochondrial Ca^{2+} transport appear to be involved in the activated Ca^{2+} transport after Ca^{2+} release.

Importance of ER Ca^{2+} Release in Activating Ca^{2+} Transport

Ryanodine was used to partially block Ca^{2+} release (McPherson and Campbell, 1993; Ogawa, 1994) in order to assess the importance of release via RyR calcium release channels in activating Ca^{2+} transport. The first caffeine pulse applied to a neuron after beginning continuous superfusion with Ringer's solution containing 20 μM ryanodine gave a $[Ca^{2+}]$ transient (not shown), but a subsequent caffeine application gave no response (Figure 5A, before peak 2). At this point ryanodine had thus markedly suppressed the effectiveness of caffeine in releasing Ca^{2+}, either by locking the channel open and (partially) depleting the ER of Ca^{2+} or by blocking the channel (Bezprozvanny et al., 1991; Nohmi et al.,

1992b). A subsequent application of 10 mM caffeine during the decay of $[Ca^{2+}]$ after high K^+ (Figure 5A, peak 2) did result in a Ca^{2+} release, even under partial block of release by ryanodine, probably due to the elevated cytosolic $[Ca^{2+}]$, which allowed 10 mM caffeine to activate Ca^{2+}-induced Ca^{2+} release (CICR; Finch et al., 1991; Hua et al., 1993, 1994; Kuba, 1994; Verkhratsky and Shmigol, 1996). However, the $[Ca^{2+}]$ transient produced by caffeine under these conditions of partial suppression of release by ryanodine was smaller than before exposure to ryanodine (peak 1) and was followed by a slow decay of $[Ca^{2+}]$ without any indication of potentiated transport. A constant, partially activated efflux pathway, leading to a shunt across the ER membrane, during the early phase of ryanodine application (Bezprozvanny et al., 1991) may have contributed to the failure of caffeine-activated Ca^{2+} release to accelerate the uptake of Ca^{2+} (peak 1). Alternatively, the significantly smaller Ca^{2+} release may not have activated RACT enough to appreciably accelerate Ca^{2+} reuptake. Subsequent applications of caffeine after later exposures to high K^+ gave smaller or no $[Ca^{2+}]$ transients (peak 3 and 4, respectively) and produced no acceleration of the rate of decline of $[Ca^{2+}]$. Thus, Ca^{2+} transport cannot be activated by caffeine itself without the large Ca^{2+} release normally produced by 10 mM caffeine in the absence of ryanodine.

Based on the above observations, the accelerated decay of $[Ca^{2+}]$ after Ca^{2+} release by caffeine appears to represent genuine stimulation of a Ca^{2+} transport mechanism into a nonmitochondrial intracellular compartment. We term this rapid Ca^{2+} transport mechanism release-activated Ca^{2+} transport (or RACT).

RACT is Thapsigargin-Insensitive

We next examined the effects of the SERCA pump inhibitor thapsigargin (TG; Thastrup et al., 1990) on the release-activated Ca^{2+} transport system. Addition of 200 nM TG to the bath caused $[Ca^{2+}]$ to increase gradually, presumably due a slow net loss of Ca^{2+} from the caffeine-sensitive Ca^{2+} store in the ER after TG block of the SERCA Ca^{2+} pump in the ER membrane (Figure 5B, before peak 2). Caffeine application after 8 min in TG caused a smaller Ca^{2+} release than before TG (peaks 2 and 1, respectively), consistent with reduced ER calcium content. A subsequent caffeine application after 15 min in 200 nM TG caused no release (not shown), suggesting that the caffeine-sensitive pool of the ER was then fully depleted of Ca^{2+}. The decay rate constant of $[Ca^{2+}]$ after peak 2 in Figure 5B was 70% of the rate before TG (0.122 and 0.192 s^{-1}, respectively, for peaks 2 and 1). Figure 5C presents the concentration dependence of the effect of TG on the relative rate constant for decay of $[Ca^{2+}]$ after caffeine from 41 neurons, in which caffeine responses were recorded both in the absence of TG and 2–10 min after application of the indicated concentration of TG. The rate constant of decay of $[Ca^{2+}]$ after caffeine was uniformly decreased to about 60% percent of control by TG concentrations ranging from 50–2000 nM. Although the concentration dependence in Figure 5C is influenced both by the TG affinity of the SERCA pump as well as the kinetics of TG permeation and compartmentalization in the neuron, the similar suppression of the Ca^{2+} uptake rate constant by 50–2000 nM TG suggests that SERCA pumps in these neurons were fully inhibited after 8–10 min in $\geqslant$50 nM TG (Thastrup et al., 1990; Bian et al., 1991; Tanaka and Tashjian, 1993). If TG inhibition of the SERCA pumps was not complete after 8–10 min at TG concentrations of 50–2000 nM, then the suppression of the uptake rate constant should have been greater at higher TG concentrations, which is contrary to the observed results. The $[Ca^{2+}]$ decay rate constant after Ca^{2+} release under these conditions of full block of SERCA pumps by TG (e.g., by 200 nM TG in Figure 5B, peak 2), was much faster than the $[Ca^{2+}]$ decay rate constant after high K^+ without Ca^{2+} release. This indicates that RACT was still activated after full block of SERCA pumps by TG, and that RACT must be mediated by a TG-insensitive mechanism. TG therefore provides a means for separating the parallel contributions of RACT and SERCA to the overall rate constant for the rapid decay of $[Ca^{2+}]$ after Ca^{2+} release. Using this approach, RACT accounts for roughly 2/3 of the combined rate constant for SERCA plus RACT when RACT is activated in the absence of TG (below).

The decay of $[Ca^{2+}]$ after high K^+ remained slow after emptying the caffeine-sensitive store by exposure to 200 nM TG (Figure 5D, peak 4). Consequently, neither caffeine alone (peak 5) nor low ER Ca^{2+} content (peak 4) was capable of activating the RACT uptake mechanism.

Rate Constants for Removal of Cytoplasmic Ca^{2+}

The inset diagram in Figure 6 illustrates the main Ca^{2+} translocation mechanisms (Miller, 1991; Pozzan et al., 1994) believed to operate in sympathetic neurons (Smith, 1994) under the conditions of our studies. Arrows pointed into the cytosolic compartment represent Ca^{2+} fluxes into the cytosol via plasma membrane voltage-sensitive Ca^{2+} channels (F_V) or via ER RyR Ca^{2+} release channels (F_{caff}). Arrows pointed out of the cytosol represent the rate constants characterizing the Ca^{2+} transport fluxes that lower $[Ca^{2+}]$ by plasma-membrane (PM) transport via the plasma membrane Ca^{2+} ATPase or the Na^+/Ca^{2+} exchanger in parallel (k_{PM}), the ER membrane SERCA pump (k_{SERCA}), and RACT (k_{RACT}). Mitochondrial Ca^{2+} fluxes have not been included in the diagram, since they do not appear to make a significant contribution to the mechanism underlying RACT.

Since the PM, SERCA, and RACT transport mechanisms act in parallel to lower $[Ca^{2+}]$ (Figure 6 insert), the overall rate constant for decay of $[Ca^{2+}]$ is the sum of the individual rate constants for each individual transport system. Thus, comparison of rates measured with various blockers or activators of different systems allows determination of the rate constants for each system (Herrington et al., 1996). To estimate values for each of the pump rates, the slow component of the decay of $[Ca^{2+}]$ after high K^+ exposure or the entire time course of decay of $[Ca^{2+}]$ after caffeine exposure was fitted by a single exponential plus constant. The corresponding rate constants were obtained as the reciprocal of the time constants of the fits, and the average values are plotted in Figure 6 for various conditions under which

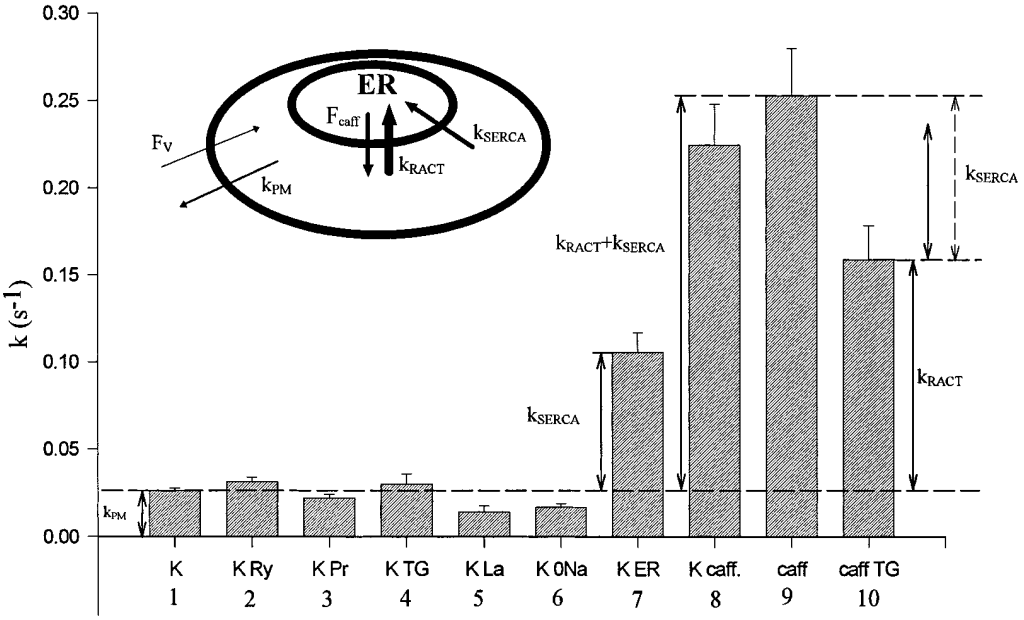

Figure 6. Decay Rate Constants of [Ca^{2+}] When Different Ca^{2+} Translocation Mechanisms Are Active

The inset shows a cell model demonstrating different Ca^{2+} translocation mechanisms. The arrows correspond to Ca^{2+} transport across the plasma membrane via ATPase, Na^+/Ca^{2+} exchanger, and permanent leak (k_{PM}); the SERCA pump (k_{SERCA}); RACT (k_{RACT}); Ca^{2+} influx through voltage-gated Ca^{2+} channels (F_V); and leak flux of Ca^{2+} through the RyR Ca^{2+} channels (F_{caff}). The bar graph shows time constants of the slow component of high K^+ responses and of the entire caffeine responses, estimated from a single exponential fit. The rate constants, calculated as the reciprocal of the time constants, are shown on the bar graph. The bars' legends correspond to the following experiments: "K" is control high K^+; "K Ry" is high K^+ in the presence of 10 or 20 μM ryanodine; "K Pr" is high K^+ in the presence of 10 mM procaine; "K TG" is high K^+ in the presence of 200–500 nM TG; "K ER" is high K^+ detected when the caffeine-sensitive Ca^{2+} pool in the ER is depleted; "K La" is high K^+ in the presence of 1 mM $LaCl_3$, which blocks the surface membrane Ca^{2+} ATPase; "K 0Na" is high K^+ detected in the absence of extracellular Na^+, to eliminate the contribution of Na^+/Ca^{2+} exchanger of the surface membrane; "K caff" corresponds to a caffeine exposure applied during [Ca^{2+}] decay after high K^+; "caff" is the caffeine-induced [Ca^{2+}] transient under control conditions; and "caff TG" is a caffeine exposure under the experimental conditions shown in Figure 5B. The number of cells used to obtain the average values represented by these bars was 14, 17, 14, 8, 5, 8, 15, 16, 14, and 16, respectively, for bars 1–10. The dashed line arrow next to column 10 is the difference between the RACT rate (k_{RACT}) and the sum of RACT and SERCA ($k_{RACT} + k_{SERCA}$) and so gives another estimation of k_{SERCA}. The solid line arrow at the left of this dashed line is the same as the isolated SERCA rate (k_{SERCA}), originally shown at the left of column 7, and serves the purpose of easier comparison between the SERCA rate determined by two different methods.

Statistically significant ($p < 0.05$) differences were found between bars 5 and 1 and between bars 6 and 1.

different Ca^{2+} transport mechanisms predominated. High K^+ was applied under control conditions (bar 1) as well as in the presence of five different blockers (bars 2–6). Block of RyR Ca^{2+} channels by ryanodine (10–20 μM; Marrion and Adams, 1992; Kuba et al., 1992; Ogawa, 1994) or procaine (10 mM; Marrion and Adams, 1992; Kuba et al., 1992) and block of SERCA pumps by TG (200–500 nM; Thastrup et al., 1990; Bian et al., 1991; Tanaka and Tashjian, 1993; Tribe et al., 1994) each had essentially no effect on the slow decay of [Ca^{2+}] after high K^+ (bars 1–4). Since RACT was not activated for the conditions represented by bars 1–4, and since the SERCA pump contribution to the slow phase of decay of [Ca^{2+}] after high K^+ was apparently balanced by an approximately opposite leak, as indicated by the lack of effect of TG on the slow phase (bars 1 and 4), the average of bars 1–4 was taken to equal the net rate constant of plasma membrane transport mechanisms (k_{PM}; dashed line). Block of PMCA by La^{3+} (bar 5) or of the plasma membrane Na^+/Ca^{2+} exchanger by Na^+-free, Ca^{2+}-free Ringer's solution (bar 6) indicated that these mechanisms each contributed significantly to k_{PM}.

Ca^{2+} was depleted from the intracellular Ca^{2+} pools by a series of caffeine exposures (usually five to six) in Ca^{2+}-free Ringer's until the cell no longer responded to caffeine. The rate constant of decay of [Ca^{2+}] after high K^+ in Ca^{2+} depleted neurons (bar 7) was larger than that attributed to k_{PM} (bars 1–4), since now Ca^{2+} uptake into the ER occurred without an opposing Ca^{2+} efflux. Thus, the full rate constant under these conditions represents $k_{SERCA} + k_{PM}$. k_{SERCA} was therefore estimated (arrow next to bar 7) as the difference between bar 7 and k_{PM}.

The rate constant of decay of [Ca^{2+}] after a caffeine response after high K^+ (bar 8) did not differ significantly from that after caffeine alone (bar 9), but was appreciably larger than the rate constant $k_{SERCA} + k_{PM}$ for decay of [Ca^{2+}] after high K^+ without caffeine but in the presence of a previously depleted Ca^{2+} pool (bar 7). The difference between the rate constants after caffeine (bars 8 and 9) and k_{PM} (bars 1–4) represents $k_{RACT} + k_{SERCA}$ (arrow next to bar 8). TG (200–500 nM) block of SERCA slowed the decay of [Ca^{2+}] after caffeine exposure (bar 10; tested under conditions shown in Figures 5B and 5C), compared to the rate after caffeine (bar 9) or after caffeine

after high K^+ (bar 8) without TG. The rate constant for the decay of $[Ca^{2+}]$ after caffeine in TG ($k_{RACT} + k_{PM}$; bar 10) was greater than the rate constant after brief K^+ depolarization of neurons with previously depleted pools ($k_{SERCA} + k_{PM}$; bar 7), indicating that RACT was greater than SERCA. The good agreement of the direct measure of $k_{RACT} + k_{SERCA}$ (arrow to the left of bar 8) and the sum of the independent, individual estimates of k_{SERCA} (arrow, bar 7) and k_{RACT} (arrow, bar 10) provide support for the rate assignments. The dashed-line arrow to the right of bar 10, which corresponds to k_{SERCA} as estimated from results after caffeine in TG, is in a good agreement with the measure of k_{SERCA} estimated from bar 7 (repeated as a solid arrow next to the dashed arrow to the right of bar 10).

A Ca^{2+} Flux Model Including RACT

The model proposed by Friel (1995) was used as a starting point for characterizing the response of cells under our conditions. Based on our present results, it was necessary to modify the original model by incorporating a mechanism which is activated by significant Ca^{2+} release from the ER and which is capable of sequestering the transported cytoplasmic Ca^{2+} without losing it from the cell. Since the delayed rise in $[Ca^{2+}]$ after RACT was caffeine-sensitive, we assumed that the new uptake mechanism is in the ER membrane and that it transfers Ca^{2+} from the cytoplasm back into the caffeine-sensitive pool. The rate constant for lowering $[Ca^{2+}]$ by the RACT transport system was assumed to be proportional to the fractional occupancy of a hypothetical regulatory Ca^{2+} binding site,

$$k_{RACT} = k_{MAX}[CaS]/([CaS] + [S]), \quad (1)$$

where k_{MAX} is the rate constant for fully activated RACT, and [S] or [CaS] is the concentration of the Ca^{2+}-free or Ca^{2+}-occupied binding site, respectively. The regulatory site was assumed to be located in close proximity to the caffeine-activated ER Ca^{2+} release channels, so that the local free Ca^{2+} concentration at the regulatory binding site ($[Ca^{2+}]_S$) was assumed to be given by

$$[Ca^{2+}]_S = [Ca^{2+}] + A \times F_{caff}, \quad (2)$$

where $[Ca^{2+}]$ is the global cytosolic free Ca^{2+} concentration, F_{caff} is the Ca^{2+} efflux rate via the caffeine-activated channels, and A is a proportionality constant relating the extra local $[Ca^{2+}]$ to the magnitude of Ca^{2+} efflux (A = 6 for the simulations presented here). The occupancy of the site is governed by numerical solution of

$$d[CaS]/dt = k_{ON}[Ca^{2+}]_S[S] - k_{OFF}[CaS], \quad (3)$$

where k_{ON} and k_{OFF} are the on and off rate constants for Ca^{2+} binding to the regulatory site S. Further details corresponding to the original Friel (1995) model and our modification are described in the Experimental Procedures.

Figure 7A reproduces several experimental conditions and observations using the computer model. In Figure 7Aa, the model parameter values (legend) were chosen to reproduce the corresponding respective peak amplitudes and time courses in the experimental data records shown in Figure 1B. The peak heights, their time course, and the amplitude and time course of the delayed $[Ca^{2+}]$ rise generated by the model all closely match the experimental records. The appearance of the secondary rise of $[Ca^{2+}]$ after Ca^{2+} release in the model arises from deactivation of the RACT transport mechanism with time after Ca^{2+} release, due to dissociation of CaS together with a Ca^{2+} overload in the ER. As observed experimentally (Figure 1), the secondary rise of $[Ca^{2+}]$ in the model with RACT was independent of extracellular Ca^{2+} concentration (not shown).

The dashed line in Figure 7Ab represents the Friel model without RACT but with all other parameter values the same as in Figure 7Aa. In the model without RACT, caffeine produces no change in the final time constant of decay of $[Ca^{2+}]$, and the $[Ca^{2+}]$ transient is not followed by a delayed rise in $[Ca^{2+}]$. It is important to note that the occurrence of a delayed rise in $[Ca^{2+}]$ cannot be reproduced by a model having time-independent values for Ca^{2+} uptake rate constants. Such a model would only produce a monotonic decay without delayed rise, as exhibited by the Friel model (1995; dashed line in Figure 7Ab). Even the inclusion of an additional uptake pool with time-independent transport rate constants, possibly representing the mitochondrial compartment, can only give a plateau during the decay of $[Ca^{2+}]$ but cannot produce a secondary rise of $[Ca^{2+}]$ (Friel and Tsien, 1994). Moreover, if SERCA pumps were sensitive to the local rather than the global $[Ca^{2+}]$, the resulting decay of $[Ca^{2+}]$ would be faster than in the Friel model (1995) but without undershoot or delayed rise of $[Ca^{2+}]$ (simulation not shown).

The simulated time course of store $[Ca^{2+}]$, during and after high K^+ (Figure 7Ac, peak 1) and during and after high K^+ followed by caffeine (Figure 7Ac, peaks 2 and 3), generated by the model with RACT for the same duration stimuli and same parameter values as used in the simulations of cytosolic $[Ca^{2+}]$ in Figure 7Aa generally reproduced the observed features in the experimental store $[Ca^{2+}]$ records for similar stimuli (Figures 2B and 2D). After minor adjustment of some of the model parameter values, the simulated store $[Ca^{2+}]$ record (Figure 7Ad) more closely reproduced the observed store $[Ca^{2+}]$ time courses in Figure 2D, and the corresponding simulated cytosolic $[Ca^{2+}]$ transient (Figure 7Ae, peak 1) for the same model parameter values and stimuli was similar to peak 1 in Figure 1D. The model with RACT can thus reproduce a range of store and cytosolic $[Ca^{2+}]$ waveforms similar to the range of responses observed during various stimuli applied to different neurons. The ability of RACT to terminate the secondary rise of cytosolic $[Ca^{2+}]$ (Figure 1D) was also duplicated by the model (Figure 7Ae, peak 2), since the second simulated caffeine application released Ca^{2+} from the same Ca^{2+} pool into which RACT pumped the Ca^{2+}.

Neurons Exhibiting RACT but No Secondary Rise of $[Ca^{2+}]$

The delayed rise of $[Ca^{2+}]$ after exposure to high K^+ and then caffeine (Figures 1, 3, 4, and 5) was observed in 86 out of 127 neurons in which caffeine was applied during the decay of $[Ca^{2+}]$ after high K^+. In Figure 7B, the final decay of $[Ca^{2+}]$ was slow after high K^+ (peak

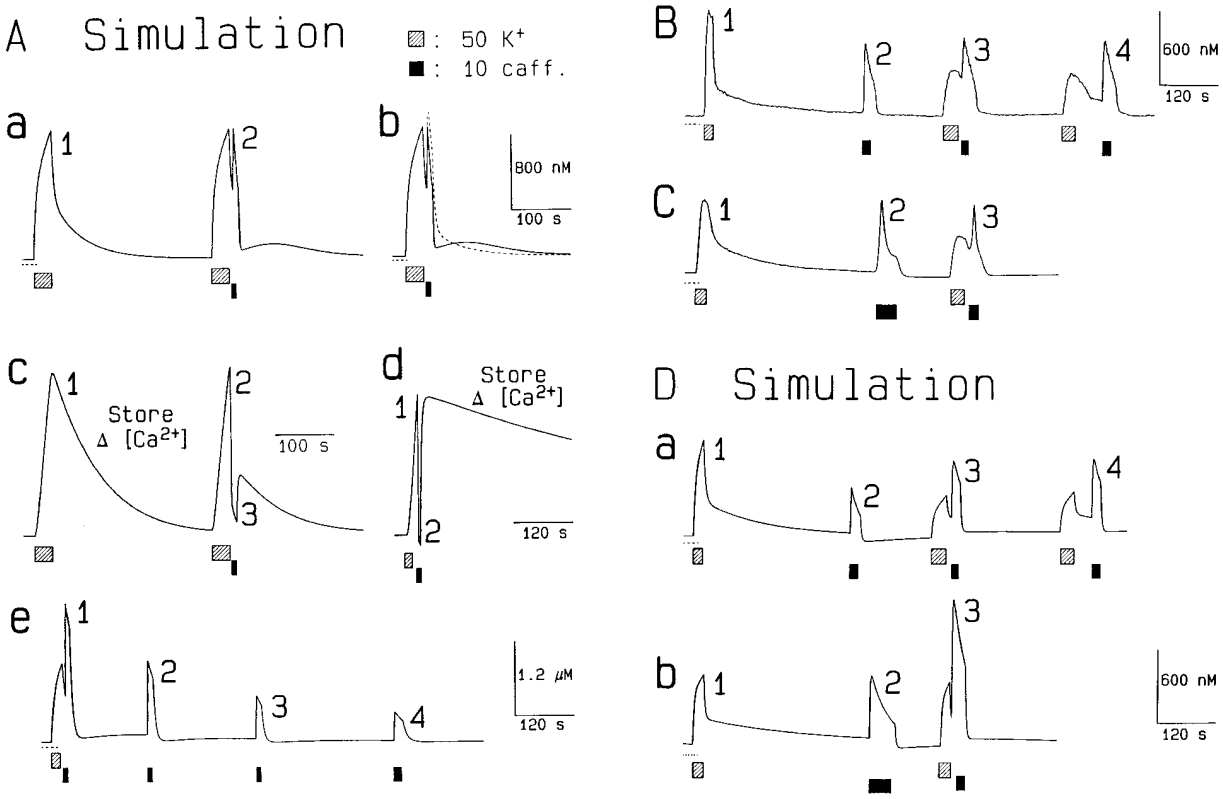

Figure 7. Response of a Mathematical Model for Neuronal Ca^{2+} Fluxes to Various High K^+ and Caffeine Pulses and Fast Ca^{2+} Uptake by RACT without Significant Delayed Rise of $[Ca^{2+}]$

(A) The Friel model (Friel, 1995) was modified, as described in the Experimental Procedures, to incorporate a Ca^{2+}-release activated fast Ca^{2+} uptake.

(a) Simulated cytosolic $[Ca^{2+}]$ calculated with the model, with parameters set to match the experimental curve shown on Figure 1B (s^{-1}): $L_m = 12 \times 10^{-7}$, $k_{PM} = 0.07$, $V_{s/c} \times L_s = 8.64 \times 10^{-3}$, $V_{s/c} \times k_{SERCA} = 0.0768$, and $V_{s/c} \times k_{MAX} = 0.172$ ($V_{s/c}$ is the ER volume ratio, set to 0.24; Friel, 1995). L_m and L_s represent Ca^{2+} leak through the plasma membrane and the ER membrane, respectively. The effect of high K^+ was simulated by increasing L_m (Friel, 1995) by a factor of 65, whereas the caffeine effect was imitated by increasing L_s (Friel, 1995) by 10. The Ca^{2+} binding and dissociation constants of the binding site activating RACT were set to $k_{ON} = 0.02\ \mu M^{-1}s^{-1}$ and $k_{OFF} = 0.02\ s^{-1}$.

(b) Simulation of peak 2 of panel (Aa) under the simulated condition that RACT is inactive (dashed line), superimposed on the simulated response when RACT is active (solid line; same as peak 2 in [Aa]). Comparison of the two curves demonstrates the effect of RACT on the time course of decay of $[Ca^{2+}]$.

(c) $[Ca^{2+}]$ changes of the caffeine-sensitive store calculated with our model involving RACT, using the same model parameter values as in panel (Aa). Simulation of the response to the same high K^+ exposure as in (Aa) (peak 1) and the response to the same exposure to high K^+ followed by a short 10 mM caffeine pulse as in (Aa) (peak 2).

(d) Simulation of store $[Ca^{2+}]$ for the indicated application of high K^+ followed by caffeine for the model involving RACT, using the same parameter values as those used in (Aa), except $k_{PM} = 0.03$, $V_{s/c} \times L_s = 2.89 \times 10^{-3}$, and $V_{s/c} \times k_{MAX} = 0.154$.

(e) RACT can terminate the delayed rise of $[Ca^{2+}]_i$ following caffeine applied after high K^+. The experimental protocol of Figure 1D was reproduced using the parameter values in (Ad), which were set to reproduce the record in Figure 1D.

(B) Exposure to high K^+ (peak 1) was followed after 5 min by an exposure to 10 mM caffeine (peak 2). Peak 3 corresponds to a high K^+ exposure followed by the immediate application of 10 mM caffeine. Peak 4 was the effect of a high K^+ exposure followed by a 60 s period of washing and application of 10 mM caffeine.

(C) Responses of another neuron, microinjected with fluo-3 (1 mM fluo-3 free acid in pipette). The first $[Ca^{2+}]$ peak was evoked by a high K^+ exposure (peak 1), while the second peak was the result of a long caffeine pulse (peak 2). The high K^+ exposure was then repeated, followed by a short caffeine pulse after a 4 s wash with Ringer's (peak 3).

(D) Simulation of responses of neurons not exhibiting a delayed rise in $[Ca^{2+}]$ after Ca^{2+} release by caffeine.

(a) Model of a cell's response to an experimental procedure similar to that shown on panel (B) of this figure. The parameter values were (s^{-1}): $L_m = 12 \times 10^{-7}$, $k_{PM} = 0.03$, $V_{s/c} \times L_s = 4.08 \times 10^{-3}$, $k_{OFF} = 0.002$, and $V_{s/c} \times k_{MAX} = 0.12$. The most important change compared to (B) was decreasing the value k_{OFF} by a factor of 10. The changes in other parameters in (Aa), (Ae), (Da), and (Db) were required to match the model peaks of high K^+ exposures to those observed in the experimental records.

(b) Computer simulation of a cell's response to a protocol similar to that shown on panel C of this figure. $L_m = 12 \times 10^{-7}$, $k_{PMCA} = 0.03$, $V_{s/c} \times L_s = 4.08 \times 10^{-3}$, $k_{OFF} = 0.002$, $V_{s/c} \times k_{MAX} = 0.12$.

1) and fast after caffeine (peak 2). Caffeine was applied at different times during the decay of $[Ca^{2+}]$ after repeated high K^+ responses (peaks 3 and 4). Each caffeine application after high K^+ caused a peak of $[Ca^{2+}]$, followed by the fast decay of $[Ca^{2+}]$ attributable to RACT, but no obvious delayed rise of $[Ca^{2+}]$ occurred in this neuron. Our computer model indicates that the rate at which RACT reverses with time after release may determine

whether or not a delayed rise in $[Ca^{2+}]$ occurs after RACT (below). Records without a delayed rise in $[Ca^{2+}]$ were also obtained from a cell microinjected with fluo-3 (potassium salt; a total of four cells were tested this way). The record in Figure 7C shows a marked acceleration of the rate of decay of $[Ca^{2+}]$ after Ca^{2+} release by caffeine (Figure 7C, peaks 2 and 3), thus demonstrating RACT using another Ca^{2+} indicator, but without a delayed rise in $[Ca^{2+}]$.

The difference in the time courses of the decay phase of $[Ca^{2+}]$ after the longer (peak 2) and shorter (peak 3) exposures to caffeine in Figure 7C indicates that Ca^{2+} was still being released at the end of the longer exposure to caffeine (Marrion and Adams, 1992). Additionally, the longer exposure to caffeine (Figure 7C, peak 2) was followed by an undershoot of $[Ca^{2+}]$ when caffeine was washed out (Friel and Tsien, 1992b; Nohmi et al., 1992b), whereas the shorter exposure (peak 3) was not (Friel and Tsien, 1992b, 1994). This observation indicates that the longer caffeine exposure, which released more Ca^{2+} from the ER, activated RACT more than the shorter exposure, which released less Ca^{2+}. Thus, the extent of activation of RACT seems to be related to the amount of Ca^{2+} released from the ER (cf. Becker et al., 1989) and is reproduced by our model (below). However, as long as the RyRs are active due to the continued presence of caffeine (above), the uptake rate of $[Ca^{2+}]$ is lower than after washing the caffeine out, because of the shunt across the ER membrane.

Simulations with RACT but without a Delayed Rise of $[Ca^{2+}]$

To eliminate the delayed rise of $[Ca^{2+}]$ from the simulated records, the rate of dissociation of Ca^{2+} from the regulatory binding site for the RACT transport system was lowered by decreasing k_{OFF}. Decreasing k_{OFF} 10-fold resulted in simulations in which caffeine pulses during the decay of $[Ca^{2+}]$ after high K^+ gave a rapid fall in $[Ca^{2+}]$ followed by only a very slow, small delayed rise (Figure 7Da), corresponding to the experimental curve in Figure 7B. When k_{OFF} is small, RACT is active for a longer period of time, providing an additional Ca^{2+} removal component which absorbs some of the Ca^{2+} entering the cytosol during the next exposure to high K^+, resulting in smaller simulated high K^+ responses (compare peak 3 or 4 with peak 1 in Figure 7Da). The records without a delayed rise of $[Ca^{2+}]$ after Ca^{2+} release obtained with microinjected fluo-3 (Figure 7C) can be similarly reproduced (Figure 7Db) by slowing the dissociation of Ca^{2+} from the regulatory binding site.

Discussion

A novel Ca^{2+} uptake mechanism, called release-activated Ca^{2+} transport or RACT, is described in this study. RACT is activated by Ca^{2+} release from ER Ca^{2+} stores but not by global elevations of Ca^{2+} caused by extracellular influx, is TG-resistant, and is not activated by depletion of Ca^{2+} stores. These observations make it likely that RACT is mediated by a Ca^{2+} translocation mechanism that is located in or near the Ca^{2+} store membrane and is distinct from the SERCA family of Ca^{2+}-ATPase molecules. RACT may serve to selectively refill intracellular Ca^{2+} stores after release, a mechanism that could be useful for repetitive responses such as oscillations of cytosolic $[Ca^{2+}]$ (Friel and Tsien, 1992a; Kuba et al., 1992; Nohmi et al., 1992b; Friel, 1995), during which the Ca^{2+} stores might otherwise become depleted. The RACT mechanism is described here in neurons, but, if present in other cell types, it could serve to conserve intracellular Ca^{2+} stores in these cells as well. For example, if RACT were activated after synchronized calcium release by voltage-clamp depolarization of cardiac myocytes, its activation and delayed deactivation would contribute to the $[Ca^{2+}]$ oscillation underlying the transient inward current (Kass et al., 1978).

RACT is activated by Ca^{2+} release from the ER but is not activated to an appreciable extent by the Ca^{2+} influx due to depolarization by elevated K^+, even though both stimuli gave rise to comparable elevations of global cytosolic $[Ca^{2+}]$. Ca^{2+} influx and Ca^{2+} release produce different spatial distributions of locally elevated $[Ca^{2+}]$ because the sites of Ca^{2+} entry into the cytoplasm are differently distributed in the two cases (Marrion and Adams, 1992). These observations suggest that the structures responsible for the activation of RACT are located near to the sites of Ca^{2+} release from the ER, where the local $[Ca^{2+}]$ is expected to be significantly higher than the globally measured $[Ca^{2+}]$ (Simon and Llinas, 1985). Proximity to the Ca^{2+} release sites ensures that RACT is activated preferentially by the elevation of local $[Ca^{2+}]$ arising from the Ca^{2+} flux during activation of Ca^{2+} release from caffeine-sensitive stores. In this way, the extent of activation of RACT is related primarily to the Ca^{2+} release flux. Once activated, however, RACT is able to remove cytoplasmic Ca^{2+} that originates from either influx or release. Rizzuto et al. (1993) reported that mitochondria located close to the ER of HeLa cells preferentially took up Ca^{2+} during activation of Ca^{2+} release. Tse et al. (1997) showed in pituitary gonadotrophs that local increase of $[Ca^{2+}]$ after Ca^{2+} release from IP_3-sensitive stores caused a 100-fold higher rate of exocytosis than that caused by a similar global increase of $[Ca^{2+}]$ due to calcium entry through the plasma membrane. Although the specific mechanism of Ca^{2+} removal from the cytoplasm and the effect of locally high $[Ca^{2+}]$ in these papers are different from those in the present experiments, the central idea, that local elevations of Ca^{2+} can activate mechanisms that are themselves spatially localized so as to respond to the Ca^{2+} release, is common.

The RACT mechanism considered here is TG-resistant, further distinguishing it from the SERCA transporter, as in the case of TG-insensitive transport mechanisms in the membranes of caffeine-sensitive stores in other cell types (Tanaka and Tashjian, 1993; Tribe et al., 1994; Herrington et al., 1996). However, we cannot rule out the possibility that RACT is generated by the SERCA pump acting in a previously unidentified mode. Previous studies of Ca^{2+} translocation in neurons of bullfrog sympathetic ganglia have not noted the possible presence of this novel Ca^{2+} transport mechanism. However, examination of previously published records does reveal a faster decline of $[Ca^{2+}]$ after Ca^{2+} release

than after Ca^{2+} influx in mouse sensory neurons (Verkhratsky and Shmigol, 1996, Figure 1C). Previous records also show that a delayed rise of $[Ca^{2+}]$ after brief caffeine application caused a rapid rise and decline of $[Ca^{2+}]$ during the slow decay of $[Ca^{2+}]$ after high K^+ in bullfrog sympathetic ganglia neurons (Friel and Tsien 1994, Figure 3e). Thus, our observations of a faster decay of $[Ca^{2+}]$ after caffeine than after high K^+ and of the delayed rise of $[Ca^{2+}]$ are not unique. However, we now present what is, to our knowledge, the first interpretation of these observations.

Magnitudes and Rates of Ca^{2+} Translocation

The Ca^{2+}-buffer capacity of cytoplasm has been estimated to be ~100, i.e., 1% of the total cytoplasmic Ca^{2+} is in the form of free ions (McBurney and Neering, 1985; Thayer and Miller, 1990; Herrington et al., 1996). Consequently, the actual rate of Ca^{2+} translocation by the main pump mechanisms must be ~100 times larger than the observed rate of decay of $[Ca^{2+}]$. However, the rate constant values shown in the Figure 6 bar graph, and thus the relative importance of the different Ca^{2+} translocation mechanisms, will not be altered by the presence of linear cytoplasmic Ca^{2+} buffers. With linear buffering of cytosolic calcium, the total calcium ($[Ca^{2+}]_T$) would be given by $[Ca^{2+}]_T = E \times [Ca^{2+}]$, where E is the buffer capacity. If E is constant, then $d[Ca^{2+}]_T/dt = E \times d[Ca^{2+}]/dt$. In this case, if $[Ca^{2+}]$ decays with a single exponential rate constant, $[Ca^{2+}]_T$ will decay with the same rate constant, but the amplitude of the change of $[Ca^{2+}]_T$ would be E times the change of $[Ca^{2+}]$. Thus, the values in our bar graph (Figure 6) would apply to the decline of both free calcium and total calcium in the case of linear buffering.

Our values for the rate constants of decay of $[Ca^{2+}]$ in neurons are comparable to those previously reported under similar conditions. Estimation of the rate constant of decay of $[Ca^{2+}]$ after high K^+, in Figure 1a of Friel and Tsien (1994), from the half-time of decay of $[Ca^{2+}]$ after ~7 s exposure to high K^+ gave a value of 0.034 s^{-1}, in close agreement with our mean value of (0.026 ± 0.001) s^{-1} for k_{PM} (Figure 6, bars 1–4). Similar analysis of Figure 4E of Friel and Tsien (1992b) gave a value of 0.13 s^{-1} for the combined rate constants for plasma membrane and ER pumps ($k_{PM} + k_{SERCA}$); again, in close agreement with our value of 0.11 ± 0.01 (Figure 6, bar 7). Finally, analysis of the decay of $[Ca^{2+}]$ after caffeine exposure (Friel and Tsien 1994, Figure 3f) gave a rate constant of 0.317 s^{-1}, which is within the range of values obtained during our studies for $k_{PM} + k_{RACT} + k_{SERCA}$ and close to our mean value of 0.25 ± 0.03 (Figure 6, bar 9). Thus, our values for rate constants of decay of $[Ca^{2+}]$ are very close to those found previously under similar conditions of stimulation. Moreover, if RACT were activated to a significant extent in the experiments of Friel and Tsien (1992b, 1994), the estimation of the contribution of SERCA pumps (k_{SERCA}) to the removal of cytosolic Ca^{2+} was overestimated by Friel (1995), perhaps by as much as 60%.

Previous studies have also reported a marked dependence of the appearance of a $[Ca^{2+}]$ plateau phase on the duration of a preceding exposure to high K^+ (Friel and Tsien, 1994). This plateau appears to be due to mitochondrial release of Ca^{2+} accumulated during the exposure to high K^+ (Friel and Tsien, 1994). In our experiments, a major contribution of mitochondria to the $[Ca^{2+}]$ transients was avoided by restricting the duration of high K^+ exposures to relatively short times (~10–12 s). Indeed, high K^+ exposures of up to 24 s in the present experiments gave only a slight indication of a plateau (e.g., Figure 4C, peak 1), attributable to mitochondrial Ca^{2+} release after uptake. This is consistent with the lack of effect of high concentrations of FCCP or CCCP on the decay of $[Ca^{2+}]$ under the stimulation conditions used here.

We have interpreted the rapid decline of cytoplasmic $[Ca^{2+}]$ after exposure to caffeine as being due to the activation of an uptake mechanism. However, it is possible that the decay of cytoplasmic $[Ca^{2+}]$ might be mediated by other processes. For example, cytoplasmic $[Ca^{2+}]$ might be rapidly reduced by the binding of Ca^{2+} to a cytoplasmic binding protein with low Ca^{2+}-affinity but high capacity, perhaps exhibiting positive cooperativity. This mechanism is untenable because such a scheme would not give a delayed rise of cytoplasmic $[Ca^{2+}]$ (Figures 1, 3, 4, and 5), but would instead exhibit a monotonic decline of $[Ca^{2+}]$ to a partially elevated level. Also, in order to account for the properties of RACT, it is necessary to envision a binding scheme with relatively low Ca^{2+} affinity ($K_D > 1$ μM) in the Ca^{2+}-free state, yet sufficiently high affinity in the Ca^{2+}-liganded states to reduce cytoplasmic Ca^{2+} back to close to the resting level. Moreover, a cytoplasmic binding protein would not discriminate between comparable elevations of $[Ca^{2+}]$ due to Ca^{2+} ions released by caffeine and Ca^{2+} entering via the plasma membrane during high K^+ depolarization, as observed here for the activation of RACT. Finally, direct monitoring of store $[Ca^{2+}]$ demonstrates rapid filling of the store when RACT is active, ruling out cytosolic Ca^{2+} binding as the mechanism for the rapid decline in cytosolic $[Ca^{2+}]$ after Ca^{2+} release.

Another possible alternative is that the rapid removal of Ca^{2+} is due not to the activation of Ca^{2+} uptake, but rather to the inactivation of a Ca^{2+} leak pathway which is significant under resting conditions but is decreased after Ca^{2+} release by caffeine. This alternative seems unlikely because exposure of neurons to ryanodine, which inactivates RyR Ca^{2+} release channels, or procaine, a nonspecific channel blocker, did not result in a significant acceleration of the decline of Ca^{2+} after exposure to elevated K^+. Finally, it was shown in Figure 5 that caffeine, an inhibitor of IP_3 receptor Ca^{2+} release channels (Ehrlich et al., 1994), did not by itself cause accelerated removal of Ca^{2+}. Thus, if such a Ca^{2+} leak pathway exists in these neurons, it is unlikely to be mediated by either a ryanodine- or IP_3-receptor Ca^{2+} release channel.

Though our model of the location and activation of RACT reproduces the experimental data quite well, the model is still a rough approximation, since the actual spatiotemporal distribution of Ca^{2+} within the cytosol and stores has not been considered. Furthermore, the molecular nature of RACT remains to be elucidated. TG-insensitivity suggests that RACT is not part of the SERCA family of Ca^{2+} pump molecules, but the proposed location of RACT suggests that RACT provides

a parallel pathway of Ca^{2+} uptake into the ER for conserving released Ca^{2+}.

Experimental Procedures

Cell Preparation and Culture

Adult frogs (Rana pipiens) were killed by decapitation and pithing. Cleaned ganglia were incubated at 35.5°C in collagenase type 1A (2.63 mg/mL; SIGMA) solution for 20 min, then transferred to a fresh collagenase solution of the same concentration for another 20 min, and finally to a trypsin solution (type III from bovine pancreas, 1.5 mg/mL; SIGMA) for 10 min. Gentle trituration of the ganglia in each solution was performed at regular 10 min intervals. All enzyme solutions were made with a 2 K^+, 0 Ca^{2+} frog Ringer's solution having the following composition: 128 mM NaCl, 2 mM KCl, 10 mM glucose, and 10 mM NaHEPES (pH 7.30 with HCl). Cells suspended in Ringer's solution were plated on micro cover glasses (VWR Scientific) coated with poly-L-lysine (SIGMA, diluted 1:10), using Petri dishes (Falcon) with 15 mm diameter openings cut from their bottoms and coverslips mounted below the opening. After the neurons were allowed to attach to the coverslips for 30–60 min, the solution was changed to culture medium consisting of a 50/50 mixture of Liebovitz's L-15 medium (Gibco BRL) and frog Ringer's solution (2 K^+, 0 Ca^{2+} Ringer's solution supplemented with 25 μg/ml ascorbic acid [Fisher], 2.5 μg/ml glutathione, 0.25 μg/ml $DMPH_4$ [both SIGMA], and 0.5 μl/ml gentamicin; pH 7.30, 280 mOsm). Cultures were stored at room temperature for up to 5 days or refrigerated for 2–6 days. Culture medium was changed every 2 days.

Single-Cell Fluorimetry and Imaging

Petri dishes were placed on the stage of a NIKON Diaphot inverted microscope. Individual cells were superfused with a custom system of computer-controlled valves (Lee Company, Essex, CT) and a 13-to-1 DAD-QMM perfusion head (Adams & List Associates, Westbury, NY). The superfusion system allowed the complete change of solution around a cell within 2 s. The Petri dish was also continuously perfused with Ringer's solution to avoid cross-contamination of nearby cells. The illumination system was a 75 W Xenon arc lamp and a computer-controlled filter wheel. Most fura-2 measurements of cytosolic $[Ca^{2+}]$ were carried out on cells loaded with 2 μM fura-2 AM (Grynkiewicz et al., 1985) for 20 min at room temperature. Cytosolic $[Ca^{2+}]$ was also monitored in some cells microinjected with fura-2 (1 mM fura-2 pentapotassium salt in pipette) or with fluo-3 (1 mM potassium salt in the injection pipette) to monitor cytosolic $[Ca^{2+}]$ without AM loading. Microinjected cells were allowed to recover for about 15 min after the injection. Store $[Ca^{2+}]$ was monitored using fluo-3FF fluorescence after loading with 4 μM fluo-3FF AM (TEFLABS, Austin, TX) for 90 min at 35°C . The detection system was a photomultiplier tube with amplifiers, detecting the emitted light at 510 nm (fura-2) or 535 nm (fluo-3 or fluo-3FF).

For fura-2 measurements of cytosolic $[Ca^{2+}]$, the ratio R of fluorescence values for excitation at 380 nm or the isosbestic wavelength 358 nm were used to calculate $[Ca^{2+}]$ as (Grynkiewicz et al., 1985)

$$[Ca^{2+}] = K_D(R - R_{MIN})/(R_{MAX} - R) \quad (4)$$

with $K_D = 135$ nM and values of R_{MAX} and R_{MIN} determined on the apparatus. R_{MAX} was determined in a group of cells by exposing them to 4 μM ionomycin (SIGMA) in Ringer's solution with 1 mM Ca^{2+}; R_{MIN} was measured in Ca^{2+}-free Ringer's solution in the presence of 4 μM ionomycin and 1 mM EGTA. Cytosolic $[Ca^{2+}]$ was calculated from fluo-3 records using

$$[Ca^{2+}] = K_D(F - F_{MIN})/(F_{MAX} - F) \quad (5)$$

with $K_D = 360$ nM (estimated from simultaneous fluo-3 and fura-2 measurements in a few of the same neurons), F as the fluorescence for excitation at 490 nm, and F_{MAX} and F_{MIN} values determined on the apparatus. To determine F_{MAX}, 8 μM 4-bromo-A23187 (SIGMA) was applied in Ringer's solution with 2 mM Ca^{2+}. F_{MIN} was calculated from the F_{MAX} value for each neuron, assuming a resting $[Ca^{2+}]$ of 80 nM. F_{MIN} was experimentally verified in a few neurons in Ca^{2+}-free Ringer's solution containing 8 μM 4-bromo-A23187 and 1 mM EGTA, prior to determining F_{MAX}. After store loading of neurons with fluo-3FF, the measured fluorescence records for excitation at 490 nm were converted to $\Delta F/F_0$, which was used as a measure of the change in $[Ca^{2+}]$ within the stores. F_0 was the fluorescence at the start of an experiment, and ΔF is $F - F_0$.

Fluorescence images of fura-2 or fluo-3FF loaded neurons were obtained using previously described procedures (Short et al., 1993) for image acquisition and removal of out of focus fluorescence by nearest neighbor deblurring.

The Student's unpaired t test was used to test significant differences ($p < 0.05$) in Figure 6.

Computer Model for Neuronal Ca^{2+} Fluxes

The model of neuronal Ca^{2+} fluxes described by Friel (1995) was used in a modified form to simulate our data. In addition to the Ca^{2+} leak and pump mechanisms introduced by Friel (1995), RACT was also built into the system as described above (Equations 1–3). The model rate constants were adjusted to reproduce the $[Ca^{2+}]$ responses of a particular neuron. The average values of the plasma membrane, SERCA, and RACT transport rate constants were determined experimentally to be 0.03, 0.08, and 0.13 s^{-1}, respectively (see Figure 6). These values were then adjusted, together with the surface and ER Ca^{2+} leak rates, according to the amplitudes and time course of the particular experimental $[Ca^{2+}]$ records to be reproduced. The differential equations were solved using a fourth order Runge-Kutta method in a custom FORTRAN program on a Gateway 2000 personal computer.

Acknowledgments

We thank Dr. D. D. Friel for helping us in starting neuron cultures and for very useful discussions of the material of this manuscript and Dr. R. W. Tsien for reading the manuscript and providing helpful suggestions for revision. We are grateful to Ms. Naima Carter for her valuable help in preparing solutions and neuron cultures and to Mr. Mark Chang for technical assistance. We also thank Gabe Sinclair and Walt Knapick for constructing mechanical components and Jeff Michael and Chuck Leffingwell for electronics support. This project was supported by a research grant from the National Institute of Neurological Disorders and Stroke (NIHER01-NS33578).

Received October 25, 1997; revised June 18, 1997.

References

Barry, V.A., and Cheek, T.R. (1994). A caffeine- and ryanodine-sensitive intracellular Ca^{2+} store can act as a Ca^{2+} source and a Ca^{2+} sink in PC12 cells. Biochem. J. *300*, 589–597.

Becker, P.L., Singer, J.J., Walsh, J.V., and Fay, F.S. (1989). Regulation of calcium concentration in voltage-clamped smooth muscle cells. Science *244*, 211–214.

Bezprozvanny, I., Watras, J., and Ehrlich, B.E. (1991). Bell-shaped calcium-response curves of Ins(1,4,5)P_3- and calcium-gated channels from endoplasmic reticulum of cerebellum. Nature *351*, 751–754.

Bian, J., Ghosh, T.K., Wang, J.-C., and Gill, D.L. (1991). Identification of intracellular calcium pools. J. Biol. Chem. *266*, 8801–8806.

Budd, S.L., and Nicholls, D.G. (1996). A reevaluation of the role of mitochondria in neuronal Ca^{2+} homeostasis. J. Neurochem. *66*, 403–411.

Butcher, R.W., and Sutherland, E.W. (1962). Adenosine 3′,5′-phosphate in biological materials. 1. Purification and properties of cyclic 3′,5′-nucleotide phosphodiesterase and use of this enzyme to characterize adenosine 3′,5′-phosphate in human urine. J. Biol. Chem. *237*, 1244–1250.

Deisseroth, K., Bito, H., and Tsien, R.W. (1996). Signaling from synapse to nucleus: postsynaptic CREB phosphorylation during multiple forms of hippocampal synaptic plasticity. Neuron *16*, 89–101.

Ehrlich, B.E., Kaftan, E., Bezprozvannaya, S., and Bezprozvanny, I. (1994). The pharmacology of intracellular Ca^{2+}-release channels. Trends Pharmacol. Sci. *15*, 145–149.

Endo, M., Tanaka, M., and Ogawa, Y. (1970). Calcium induced release of calcium from the sarcoplasmic reticulum of skinned skeletal muscle fibers. Nature *228*, 34–36.

Finch, E.A., Turner, T.J., and Goldin, S.M. (1991). Calcium as a coagonist of inositol 1,4,5-triphosphate-induced calcium release. Science *19*, 443–446.

Friel, D.D. (1995). $[Ca^{2+}]_i$ oscillations in sympathetic neurons: an experimental test of a theoretical model. Biophys. J. *68*, 1752–1766.

Friel, D.D., and Tsien, R.W. (1992a). Phase-dependent contributions from Ca^{2+} entry and Ca^{2+} release to caffeine-induced $[Ca^{2+}]_i$ oscillations in bullfrog sympathetic neurons. Neuron *8*, 1109–1125.

Friel, D.D., and Tsien, R.W. (1992b). A caffeine-and ryanodine-sensitive Ca^{2+} store in bullfrog sympathetic neurones modulates effects of Ca^{2+} entry on $[Ca^{2+}]_i$. J. Physiol. *450*, 217–246.

Friel, D.D., and Tsien, R.W. (1994). An FCCP-sensitive Ca^{2+} store in bullfrog sympathetic neurons and its participation in stimulus-evoked changes in $[Ca^{2+}]_i$. J. Neurosci. *14*, 4007–4024.

Ginty, D.D. (1997). Calcium regulation of gene expression: Isn't that spatial? Neuron *18*, 186–193.

Golovina, V.A., and Blaustein, M.P. (1997). Spatially and functionally distinct Ca^{2+} stores in sarcoplasmic and endoplasmic reticulum. Science *275*, 1643–1648.

Grynkiewicz, G., Poenie, M., and Tsien, R.Y. (1985). A new generation of Ca^{2+} indicators with greatly improved fluorescence properties. J. Biol. Chem. *260*, 3440–3450.

Gunter, T.E., and Pfeiffer, D.R. (1990). Mechanisms by which mitochondria transport calcium. Am. J. Physiol. *258*, C755-C786.

Hehl, S., Golard, A., and Hille, B. (1996). Involvement of mitochondria in intracellular calcium sequestration by rat gonadotropes. Cell Calcium *20*, 515–524.

Herrington, J., Park, Y.B., Babcock, D.F., and Hille, B. (1996). Dominant role of mitochondria in clearance of large Ca^{2+} loads from rat adrenal chromaffin cells. Neuron *16*, 219–228.

Herrmann-Frank, A., Richter, M., Sarkozi, S., Mohr, U., and Lehmann-Horn, F. (1996). 4-chloro-*m*-cresol, a potent and specific activator of the skeletal muscle ryanodine receptor. Biochim Biophys Acta *1289*, 31–40.

Hofer, A.M., and Machen, T.E. (1993). Technique for in situ measurements of calcium in intracellular inositol 1,4,5-tris-phosphate-sensitive stores using the fluorescent indicator mag-fura-2. Proc. Natl. Acad. Sci. USA *90*, 2598–2602.

Hua, S.-Y., Nohmi, M., and Kuba, K. (1993). Characteristics of Ca^{2+} release induced by Ca^{2+} influx in cultured bullfrog sympathetic neurones. J. Physiol. *464*, 245–272.

Hua, S.-Y., Tokimasa, T., Takasawa, S., Furuya, Y., Nohmi, M., Okamoto, H., and Kuba, K. (1994). Cyclic ADP-ribose modulates Ca^{2+} release channels for activation by physiological Ca^{2+} entry in bullfrog sympathetic neurons. Neuron *12*, 1073–1079.

Huang, W.-C., and Chueh, S.-H. (1996). Calcium mobilization from the intracellular mitochondrial and nonmitochondrial stores of the rat cerebellum. Brain Res. *718*, 151–158.

Kao, J.P.Y. (1994). Practical aspects of measuring $[Ca^{2+}]$ with fluorescent indicators. Methods Cell Biol. *40*, 155–181.

Kass, R.S., Lederer, W.J., Tsien, R.W., and Weingart, R. (1978). Role of calcium ions in transient inward currents and aftercontractions induced by strophanthidin in cardiac Purkinje fibres. J. Physiol. *281*, 187–208.

Kuba, K. (1994). Ca^{2+}-induced Ca^{2+} release in neurones. Jpn. J. Physiol. *44*, 613–650.

Kuba, K., Nohmi, M., and Hua, S.-Y. (1992). Intracellular Ca^{2+} dynamics in response to Ca^{2+} influx and Ca^{2+} release in autonomic neurones. Can. J. Physiol. Pharmacol. *70*, S64-S72.

Le Guennec, J.-Y., Lacamapagne, A., and Garnier, D. (1996). Orthophosphate salts induce calcium current recovery from blockade by gadolinium in isolated guinea-pig ventricular myocytes. Exp. Physiol. *81*, 577–585.

Lipscombe, D., Madison, D.V., Poenie, M., Reuter, H., Tsien, R.W., and Tsien, R.Y. (1988). Imaging of cytosolic Ca^{2+} transients arising from Ca^{2+} stores and Ca^{2+} channels in sympathetic neurons. Neuron *1*, 355–365.

Marrion, N.V., and Adams, P.R. (1992). Release of intracellular calcium and modulation of membrane currents by caffeine in bull-frog sympathetic neurones. J. Physiol. *445*, 515–535.

McBurney, R.N., and Neering, V. (1985). The measurements of changes in intracellular free calcium during action potentials in mammalian neurones. J. Neurosci. Methods *13*, 65–76.

McPherson, P.S., and Campbell, K.P. (1993). Characterization of the major brain form of the ryanodine receptor/Ca^{2+} release channel. J. Biol. Chem. *268*, 19785–19790.

Miller, R.J. (1991). The control of neuronal Ca^{2+} homeostasis. Prog. Neurobiol. *37*, 255–285.

Müller, C.E., and Daly, J.W. (1993). Stimulation of calcium release by caffeine analogs in pheochromocytoma cells. Biochem. Pharmacol. *46*, 1825–1829.

Nohmi, M., Hua, S.-Y., and Kuba, K. (1992a). Intracellular calcium dynamics in response to action potentials in bullfrog sympathetic ganglion cells. J. Physiol. *458*, 171–190.

Nohmi, M., Hua, S.-Y., and Kuba, K. (1992b). Basal Ca^{2+} and the oscillation of Ca^{2+} in caffeine-treated bullfrog sympathetic neurones. J. Physiol. *450*, 513–528.

Ogawa, Y. (1994). Role of ryanodine receptors. Crit. Rev. Biochem. Mol. Biol. *29*, 229–274.

Palade, P. (1987). Drug induced Ca^{2+} release from isolated sarcoplasmic reticulum. J. Biol. Chem. *262*, 6142–6148.

Pozzan, T., Rizzuto, R., Volpe, P., and Meldolesi, J. (1994). Molecular and cellular physiology of intracellular calcium stores. Physiol. Rev. *74*, 595–636.

Rizzuto, R., Bastianutto, C., Brini, M., Murgia, M., and Pozzan, T. (1994). Mitochondrial Ca^{2+} homeostasis in intact cells. J. Cell Biol. *126*, 1183–1194.

Rizzuto, R., Brini, M., Murgia, M., and Pozzan, T. (1993). Microdomains with high Ca^{2+} close to IP_3-sensitive channels that are sensed by neighboring mitochondria. Science *262*, 744–747.

Rousseau, E., LaDine, J., Liu, Q.-Y., and Meissner, G. (1988). Activation of the Ca^{2+} release channel of skeletal muscle sarcoplasmic reticulum by caffeine and related compounds. Arch. Biochem. Biophys. *267*, 75–86.

Short, A.D., Klein, M.G., Schneider, M.F., and Gill, G.L. (1993). Inositol 1,4,5-tris-phosphate-mediated quantal Ca^{2+} release measured by high resolution imaging of Ca^{2+} within organelles. J. Biol. Chem. *268*, 25887–25893.

Simon, S.M., and Llinas, R.R. (1985). Compartmentalization of the submembrane calcium activity during calcium influx and its significance in transmitter release. Biophys. J. *48*, 485–498.

Smith, P.A. (1994). Amphibian sympathetic ganglia: an owner's and operator's manual. Prog. Neurobiol. *43*, 439–510.

Tanaka, Y., and Tashjian, A.H. (1993). Functional identification and quantitation of three intracellular calcium pools in GH_4C_1 cells: evidence that the caffeine-responsive pool is coupled to a thapsigargin-resistant, ATP-dependent process. Biochemistry *32*, 12062–12073.

Terasaki, M., and Sardet, C. (1991). Demonstration of calcium uptake and release by sea urchin egg cortical endoplasmic reticulum. J. Cell Biol. *115*, 1031–1037.

Thastrup, O., Cullen, P.J., Drobak, B.K., Hanley, M.R., and Dawson, A.P. (1990). Thapsigargin, a tumor promoter, discharges intracellular Ca^{2+} stores by specific inhibition of the endoplasmic reticulum Ca^{2+} ATPase. Proc. Natl. Acad. Sci. USA *87*, 2466–2470.

Thayer, S.A., and Miller, R.J. (1990). Regulation of the intracellular free calcium concentration in single rat dorsal root ganglion neurones in vitro. J. Physiol. *425*, 85–115.

Tribe, R.M., Borin, M.L., and Blaustein, M.P. (1994). Functionally and spatially distinct Ca^{2+} stores are revealed in cultured vascular smooth muscle cells. Proc. Natl. Acad. Sci. USA *91*, 5908–5912.

Tse, F.W., Tse, A., Hille, B., Horstmann, H., and Almers, W. (1997). Local Ca^{2+} release from internal stores controls exocytosis in pituitary gonadotrophs. Neuron *18*, 121–132.

Verkhratsky, A., and Shmigol, A. (1996). Calcium-induced calcium release in neurones. Cell Calcium *19*, 1–14.

Zidichousky, J.A., Kehoe, M.P., Wong, K., and Smith, P.A. (1989). Elevation of intracellular cyclic AMP concentration fails to inhibit adrenaline-induced hyperpolarization in amphibian sympathetic neurones. Br. J. Pharmacol. *96*, 779–784.

Zorzato, F., Scutari, E., Tegazzini, V., Clementi, E., and Treves, S. (1993). Chlorocresol: An activator of ryanodine receptor-mediated Ca^{2+} release. Mol. Pharmacol. *44*, 1192–1201.